Journal of Vertebrate Paleontology 30(3):911–927, May 2010

ARTICLE

REVISITING THE INTERTROPICAL BRAZILIAN SPECIES *HOPLOPHORUS EUPHRACTUS* (CINGULATA, GLYPTODONTOIDEA) AND THE PHYLOGENETIC AFFINITIES OF *HOPLOPHORUS*

KLEBERSON de O. PORPINO,*[1,3] JUAN C. FERNICOLA,[2] and LÍLIAN P. BERGQVIST[3]
[1]Departamento de Ciências Biológicas, Universidade do Estado do Rio Grande do Norte, Rua Antônio Campos s/n, Mossoró 59610-090, Rio Grande do Norte, Brazil, kleporpino@yahoo.com.br;
[2]Sección Paleontología de Vertebrados, Museo Argentino de Ciencias Naturales "Bernardino Rivadavia," Av. Ángel Gallardo 470, C1405DJR, Buenos Aires, Argentina, jctano@macn.gov.ar;
[3]Departamento de Geologia/UFRJ, Av. Athos da Silveira Ramos, 274, CCMN, bloco G, Cidade Universitária, 21941-916, Rio de Janeiro/RJ, Brazil, bergqvist@geologia.ufrj.br

ABSTRACT—The genus *Hoplophorus* is one of the most distinctive glyptodonts from the Quaternary deposits of the intertropical area of Brazil. In this paper, we redescribe cranial and postcranial elements and describe some new tarsal elements belonging to the species *Hoplophorus euphractus* from caves from Minas Gerais state, southern Brazil, in order to provide a better diagnosis for the genus. The material examined shows several striking, distinctive characters relative to *Neosclerocalyptus*, besides those previously reported, reinforcing the validity of *Hoplophorus*. On the other hand, we find that the postcrania of *Hoplophorus* presents striking, unreported resemblances with *Panochthus* (e.g., more lateromedially elongated cuboid facet of navicular and caudal tube with large lateral figures separated from the terminal ones by a wide space). In order to infer the relationships of *Hoplophorus* and to reevaluate the monophyly of the tribe Hoplophorini and the subfamily Hoplophorinae (in which *Hoplophorus* was previously allocated), we carried out a cladistic analysis of 18 taxa, including 13 glyptodont genera and five cingulate outgroups, scored for 151 cranial, dental, and postcranial characters. The most parsimonious tree shows that Hoplophorinae and Hoplophorini are both paraphyletic and has *Hoplophorus* as the sister group to *Panochthus* based mostly on synapomorphies of the caudal tube. We propose: (1) restricting the definition of the tribe Hoplophorini to the lineage represented by *Hoplophorus*, making it the sister group to Panochthini within Panochthinae (= *Hoplophorus* + *Panochthus*); and (2) a new subfamily, Neosclerocalyptinae, represented by *Neosclerocalyptus,* the sister group to Panochthinae.

INTRODUCTION

Hoplophorus is a medium-sized glyptodont genus known from the late Pleistocene of the Brazilian intertropical area (sensu Cartelle, 1999). *Hoplophorus euphractus*, its type species, was erected by Lund (1839) on the basis of osteoderms and carapace fragments from Pleistocene cave deposits of Lagoa Santa region, Minas Gerais state, and was one of the earliest described glyptodonts (Ameghino, 1889). In addition to the osteoderms, Lund attributed to *H. euphractus* several limb bones (Lund, 1840a), teeth, vertebrae (Lund, 1842), and an incomplete skull and foot (Lund, 1846) collected in the same cave as the type material (Lapa do Baú; Winge, 1915). Besides *H. euphractus,* Lund proposed three additional species of *Hoplophorus* based on material from Lagoa Santa region, but their validity was seriously questioned by later authors. *Hoplophorus selloi* was proposed by Lund in 1840 (Lund 1840a), but was actually based on remains belonging to *Glyptodon clavipes* and *Dasypus sulcatus* (= *Propraopus sulcatus*), as demonstrated by Winge (1915). Lund (1840b) mentioned a small species of *Hoplophorus* for which he coined the name *Hoplophorus minor*, but he did not presented any description or illustration, and this taxon was subsequently attributed to the genus *Glyptodon* by Ameghino (1889) and later considered a synonym of *H. euphractus* by Winge (1915) and Paula Couto (1957). *Hoplophorus meyeri* (Lund, 1844), the last species erected by Lund, is presently considered a nomen nudum because it was not described nor defined (Winge, 1915; Paula Couto, 1947). In fact, the same also should apply to *H. minor* and *H. selloi*, as they were neither defined nor described (ICZN, 1999).

Pouchet (1866) regarded the species *Glyptodon ornatus*, erected by Owen (1845) on the basis of carapace fragments collected in Argentina, as a synonym of *H. euphractus*. He also attributed to *H. euphractus* a complete carapace and postcranial bones from Argentina housed in the collection of the Natural History Museum of Paris (Pouchet, 1866). Based on new Pampean specimens and reevaluation of the material described by Owen (1845) and Pouchet (1866), Burmeister (1870–74) argued for the inclusion of *G. ornatus* within *Hoplophorus*, as did Pouchet (1866), but in a species distinct from *H. euphractus* (sensu Lund 1839), for which he coined the new combination *Hoplophorus ornatus.* After that, Ameghino (1889) added several species from the Pampean region of Argentina and Uruguay to *Hoplophorus*, but in 1891 he proposed the new name *Sclerocalyptus* as a nomen novum (ICZN 1999, Art 67.8) to replace *Hoplophorus*, arguing that it was preoccupied by *Oplophores* (Pisces), *Hoplophora* (Insecta), and *Oplophorus* (Crustacea) (Ameghino, 1891), and designated *G. ornatus* as its type species. When revising the material collected by Lund (1839), Winge (1915) questioned the inclusion of *H. euphractus* within *Sclerocalyptus* (sensu Ameghino, 1891), based on its distinctive morphology relative to the Pampean species also included in this genus.

Simpson (1945) noted that the decision of Ameghino (1891) was incorrect, since just a single letter difference is enough to avoid homonymy at the generic level (ICZN 1999, Art. 56.2), and therefore that *Hoplophorus* was not preoccupied. As more

---

*Corresponding author.

complete material became available, including a carapace, a nearly complete caudal tube, and better preserved cranial and postcranial material (Paula Couto, 1947, 1957), the differences between *H. euphractus* and the Pampean species with which it previously had been allied became more evident, leading Paula Couto (1957) to officially recognize the Brazilian taxon as belonging to a distinct genus, as already suggested by Winge (1915). Therefore, considering that *H. euphractus* is the proper type species of *Hoplophorus* (and not *G. ornatus* as believed by Ameghino, 1889) and that "*Sclerocalyptus*" is a junior synonym of this latter genus (Simpson, 1945), Paula Couto (1957) conserved the name *Hoplophorus* for the Brazilian taxa and proposed the new name *Neosclerocalyptus* to encompass all species other than *H. euphractus* that were included in "*Sclerocalyptus*" (sensu Ameghino, 1891) (see Zurita et al., 2007, and Fernicola, 2008, for additional discussions).

In addition to the intertropical Brazilian area, remains attributed to *Hoplophorus* have been reported from the Pleistocene of Acre state, north Brazil (Paula Couto, 1983), and from the Pleistocene of Bolivia (Hoffstetter, 1964; Zurita et al., 2009). The material from Bolivia was tentatively attributed to a new species, *Hoplophorus echazui*, by Hoffstetter (1964), but its validity is uncertain since it was based on sparse and poorly diagnostic material (Zurita et al., 2009).

Hoplophorus has been placed in the subfamily Hoplophorinae (Paula Couto, 1957) within the tribe Hoplophorini (Hoffstetter, 1958; McKenna and Bell, 1997), though this genus presents some highly distinctive characters relative to the other alleged members of this tribe, as already noted by Hoffstetter (1958). Hoplophorinae is a large but loosely defined group (Hoffstetter, 1958) that encompasses most described glyptodonts (nearly 60% of the known genera according to McKenna and Bell, 1997). The monophyly of this group recently has been questioned (Fernicola, 2008).

We here redescribe the material of *H. euphracutus* studied by Paula Couto (1957) and describe new tarsal elements for this species, focusing on further clarification of valuable anatomical characters not detailed by previous authors (Winge, 1915; Paula Couto, 1957), in order to provide a robust differential diagnosis for *Hoplophorus*. In addition, we carry out a cladistic analysis: (1) to access the relationships of *Hoplophorus*; (2) to revaluate its previous assignment to Hoplophorinae and Hoplophorini (as suggested by previous authors; Paula Couto, 1957; Hoffstetter, 1958; McKenna and Bell, 1997); and (3) to provide a new test of the phylogenetic status of these latter groups.

Institutional Abbreviations—**MACN**, Museo Argentino de Ciencias Naturales "Bernardino Rivadavia," Buenos Aires, Argentina; **MCC**, Museu Câmara Cascudo, Natal/RN, Brazil; **MCL**, Museu de Ciências Naturais da Pontifícia Universidade Católica de Minas Gerais, Belo Horizonte/MG, Brazil; **MHN**, Museu de História Natural e Jardin Botânico, Belo Horizonte/MG, Brazil; **MLP**, Museo de Ciencias Naturales de La Plata, La Plata, Argentina; **MNRJ**, Museu Nacional do Rio de Janeiro, Rio de Janeiro/RJ, Brazil; **FC-DPV**, Colección de Vertebrados Fósiles, Faculdad de Ciencias, Universidad de la República, Uruguay.

Other Abbreviations—**CI**, consistency index; **RI**, retention index.

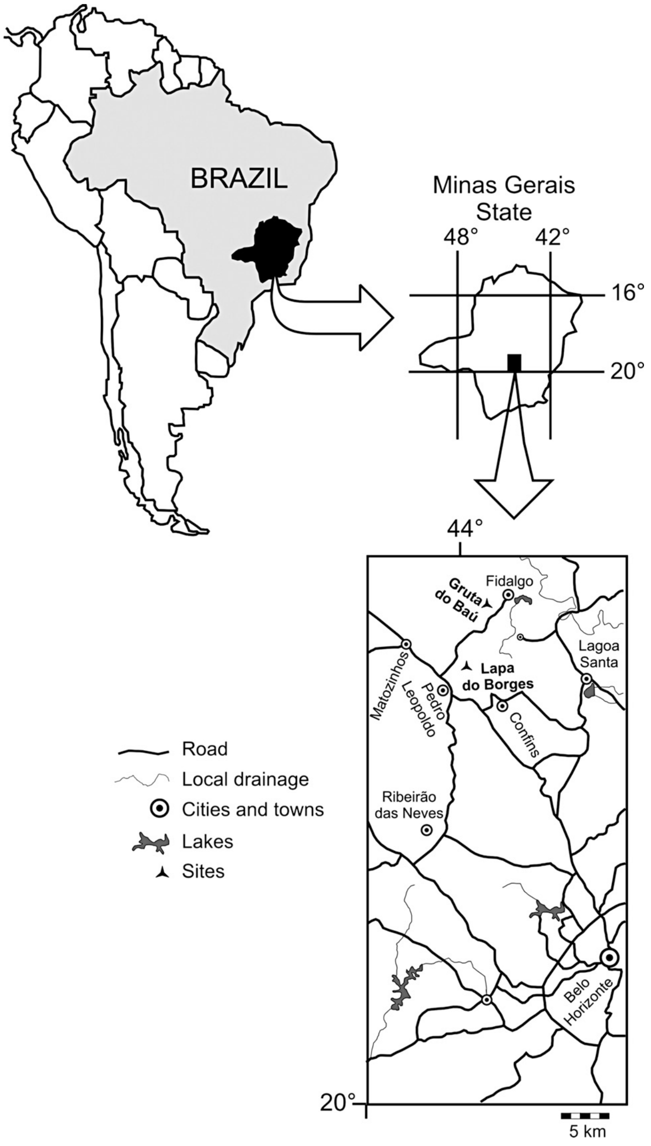

FIGURE 1. Location map of Gruta do Baú and Lapa do Borges.

MATERIAL AND METHODS

Most of the specimens here studied were previously described by Paula Couto (1947, 1957) and were collected in carbonate caves at Lapa do Borges, Pedro Leopoldo city, Minas Gerais state, Brazil (Fig. 1). This material includes a fragmented skull, several paired postcranial elements, isolated osteoderms, a caudal tube, and a partial carapace that, according to Paula Couto (1947, 1957), were found in association and probably belonged to a single individual. These specimens are stored in the collection of MHN. In addition, we describe unpublished tarsal elements from Gruta do Baú, Minas Gerais state (Fig. 1). This material belongs to the fossil mammal collection of MCL and was collected in association with osteoderms. Available radiometric ages for the fossils collected in caves from the Lagoa Santa region range from 9,130 ± 150 years BP (Auler et al., 2006; Neves and Piló, 2003) to 77,700 ± 6,100 years BP (Gruta do Baú; Piló, 1998). For this reason, we assign the material here described to the late Pleistocene–early Holocene.

In this paper we use dorsal, lateral, and marginal to refer to regions of the carapace. We adopt the usually employed terms 'lateral figures' and 'terminal figures' to denote the paired larger elliptical figures at the sides and distal end of the caudal tube, respectively (see Castellanos, 1939, 1941; Cabrera, 1944). In describing individual osteoderms we follow primarily the terminology employed by Hill (2006), but we prefer to use 'main figure' in reference to the larger figure in the external ornamentation of osteoderms instead of 'central figure' because in some glyptodontid species (e.g., *Parapropalaehoplophorus*) it does not occupy a

TABLE 1. Measurements (mm) of the skull of *Hoplophorus euphractus* MHN 992.

Measurements	
Length	336
Width at the postorbital processes	142
Width at the postorbital constriction	101
Width of foramen magnum	38
Height of foramen magnum	30
Width between occipital condyles	96.7
Maximum width of basioccipital	74.5
Maximum width of basisphenoid	42.5
Length of basisphenoid	62
Width between oval foramina	58
Width between sphenorbital fissures	35.3

central position (Croft et al., 2007). We use M to indicate upper molariforms in accordance to the current literature (e.g., Perea, 2005; Croft et al., 2007). Details on the phylogenetic methods employed are given in the Phylogenetic Analysis section. The comparative descriptions were based mostly on direct observations of specimens and on published accounts listed in Appendix 1. Selected measurements are provided for cranial (Table 1) and postcranial elements (Table 2). In the Systematic Paleontology section, we followed the classification of glyptodonts recently proposed by Fernicola (2008).

SYSTEMATIC PALEONTOLOGY

Order CINGULATA Illiger, 1811
Suborder GLYPTODONTIA Ameghino, 1889
Superfamily GLYPTODONTOIDEA Gray, 1869
Family PANOCHTHIDAE Castellanos, 1927
Genus *HOPLOPHORUS* Lund, 1839
(= *Sclerocalyptus* Ameghino, 1891)

Revised Diagnosis—Differs from all known glyptodonts (except from *Panochthus* and *Neuryurus*) in having conical tubercles in lateral and terminal figures of caudal tube. Differs further from all known glyptodonts (except *Urotherium* and *Doedicurus*) in having single lateral figure in each side of caudal tube and in having lateral figures with dorsoventral diameter nearly matching dorsoventral diameter of caudal tube in its corresponding position (except from Panochthini). Differs from *Neuryurus* in having carapace and caudal tube osteoderms with clearly demarcated main and peripheral figures (instead of perforated, without any discernable figure) and in having firmly attached osteoderms in the caudal tube (instead of poorly attached). Differs from its closer allies *Neosclerocalyptus* and *Panochthus* in having: nearly rounded osteoderms in dorsal region of carapace (instead of pentagonal or hexagonal); narrower glenoid fossa; elongated humeral head (instead of rounded); medial and lateral proximal borders of patella nearly symmetrical and not projecting proximally; and more proximodistally elongated sustentacular facet of astragalus. Differs further from *Panochthus* in having main figures in all carapace osteoderms. Differs further from *Neosclerocalyptus* in being larger and in having osteoderms from the dorsal region of carapace with two rows of peripheral figures (instead of a single row).

TABLE 2. Measurements (mm) of postcranial elements of *Hoplophorus euphractus.*

Measurements	Specimens		
Scapula	MHN 985	MHN 984	Winge (1915)
Length of glenoid fossa	79	78.4	—
Maximum width of glenoid fossa	43	43	—
Humerus	MHN 987	MHN 996	
Length	332	330	329
Distal width	99	100	
Width of distal articular surface	62	62	59
Length of deltopectoral shelf	167	168	
Femur	MHN 988		
Distal width	165		
Patella	MHN 990	MHN 989	
Length	86	87	80/77/76
Width	80.3	80.6	75/72
Astragalus	MCL 21.107		
Length	70.8		67/65
Width	79.6		
Length of ectal facet	51.4		
Length of sustentacular facet	41.6		

HOPLOPHORUS EUPHRACTUS Lund, 1839
(Figs. 2–7)

Diagnosis—As for genus.

Studied Material—MHN 992, incomplete skull; MHN 993–1001, teeth; MHN 755, palate fragment; MHN 984, left scapula; MHN 985, right scapula; MHN 986, left humerus; MHN 987, right humerus; MHN 988, distal half of right femur; MHN, 989 left patella; MHN 990, right patella; MHN 1003 partial carapace, MHN 1004, fragment from the lateral region of carapace; MHN 1005, caudal tube; MCL 21.107, left astragalus; MCL 21.108, left navicular.

DESCRIPTIONS AND COMPARISONS

Carapace—As in *Neosclerocalyptus*, the carapace osteoderms (Fig. 2A–D) are thinner than in larger Pleistocene genera such as *Glyptodon* and *Panochthus.* As in *Glyptodon* and some species within *Neosclerocalyptus*, transverse rows of osteoderms are more noticeable at the lateral sides of carapace than in the dorsal region, unlike *Panochthus*, where they are visible along the entire carapace. The osteoderm surface is more rugose and punctuated than in *Neosclerocalyptus*, somewhat like in *Glyptodon* and *Panochthus*, with a flat to moderately concave main figure. As in *Neosclerocalyptus*, the main and peripheral sulci are shallower and less marked than in *Glyptodon*. The osteoderms from the dorsal region are nearly rounded (instead of pentagonal or hexagonal, as in *Panochthus* and *Neosclerocalyptus*) with a circular, centrally positioned main figure (Fig. 2C). As in *Neosclerocalyptus* and *Panochthus*, the lateral osteoderms are hexagonal or pentagonal, with the major axis oriented anteroposteriorly (Fig. 2B, D), except the posterior-most, which are nearly isodiametric. The osteoderms near the lateral margins are almost quadrangular, and have a subelliptical main figure that is proportionally larger than in all dorsal and most lateral osteoderms. The peripheral figures, numbered 9–12, are relatively smaller than in *Neosclerocalyptus*, and are polygonal or nearly rounded. Unlike in *Neosclerocalyptus*, some osteoderms of the central and anterior portions of the dorsal region bear two rows of peripheral figures, as in some hoplophorines such as *Plohophorus* and *Stromaphorus*, but this occurs in fewer areas than in these latter genera.

Caudal Ring—The diameter (nearly 133 mm) of the nearly complete caudal ring (MHN 209-210; Fig. 2I) matches the distance between the lateral edges of the transverse processes of the eighth vertebra (132 mm). This led Paula Couto (1957) to infer that MHN 209-210 corresponds to the last of a sequence of at least eight rings, each presumably covering one single caudal vertebra. Following this inference, *Hoplophorus* would have slightly more caudal rings than *Panochthus* (six to seven; Burmeister, 1870–74) and many more than *Neosclerocalyptus* (four to five; Burmeister, 1870–74). The number of caudal rings nearly matches the number of caudal vertebrae in *Panochthus*

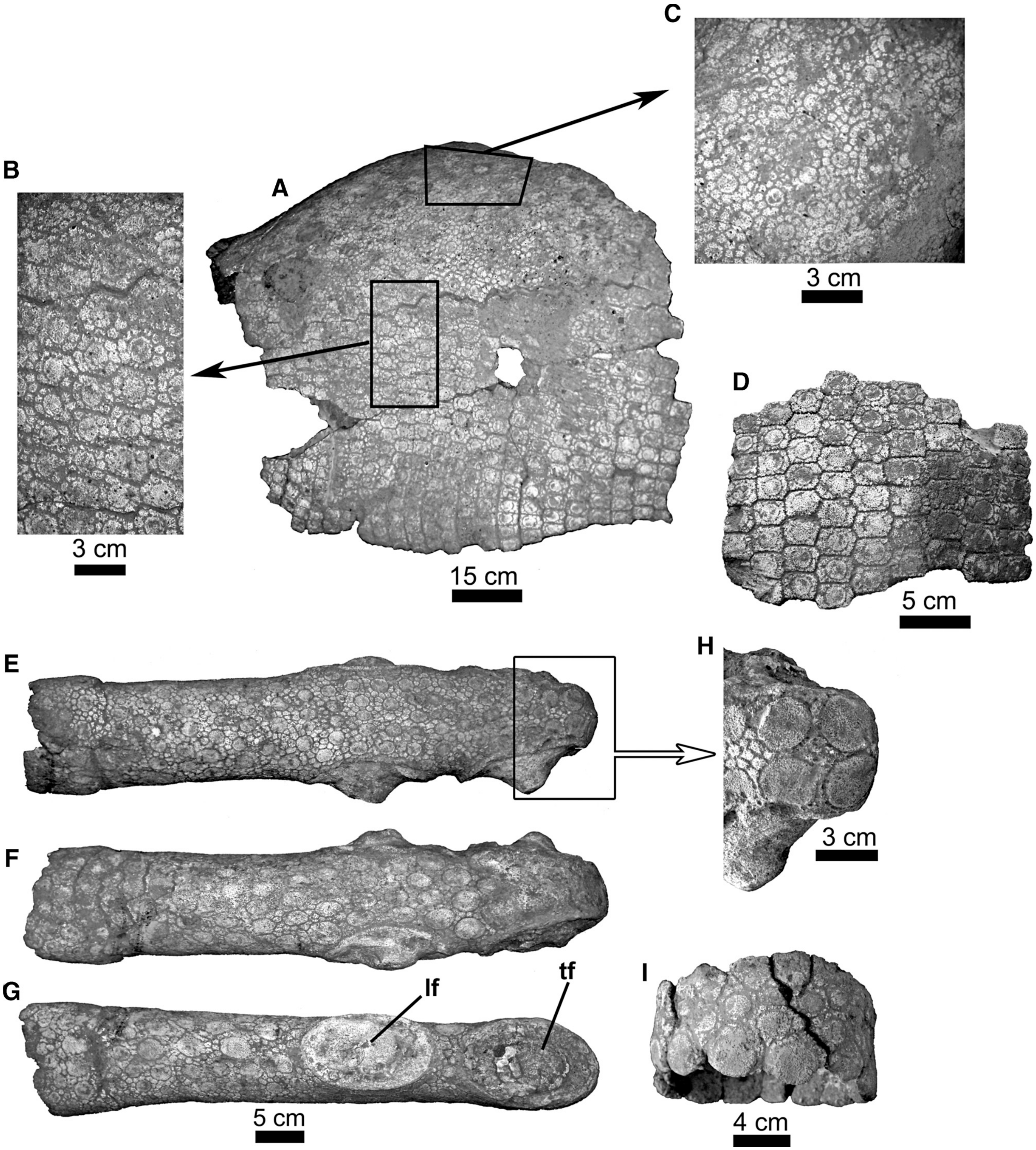

FIGURE 2. Carapace and caudal armor of *Hoplophorus euphractus.* **A**, incomplete carapace MHN 1003 in lateral view; **B**, detail showing lateral osteoderms; **C**, detail showing dorsal osteoderms; **D**, fragment of lateral region MHN 1004; **E**, caudal tube MHN 1005 in dorsal view; **F**, caudal tube MHN 1005 in ventral view; **G**, caudal tube MHN 1005 in lateral view; **H**, detail of the distal end of caudal tube MHN 1005 in dorsal view; **I**, eighth caudal ring MHN 209-210 in caudal view. **Abbreviations**: **lf**, lateral figure; **tf**, terminal figure.

(six rings to seven vertebrae) but this is not true for *Neosclerocalyptus* (four to five rings for seven vertebrae). This indicates that the number of caudal rings and the number of caudal vertebrae anterior to the caudal tube do not necessarily match each other in closely allied genera and, consequently, we remain cautious regarding the reconstruction proposed by Paula Couto (1957:fig. 30). Unlike *Panochthus* and *Neosclerocalyptus*, which present two and two to three rows of osteoderms, respectively,

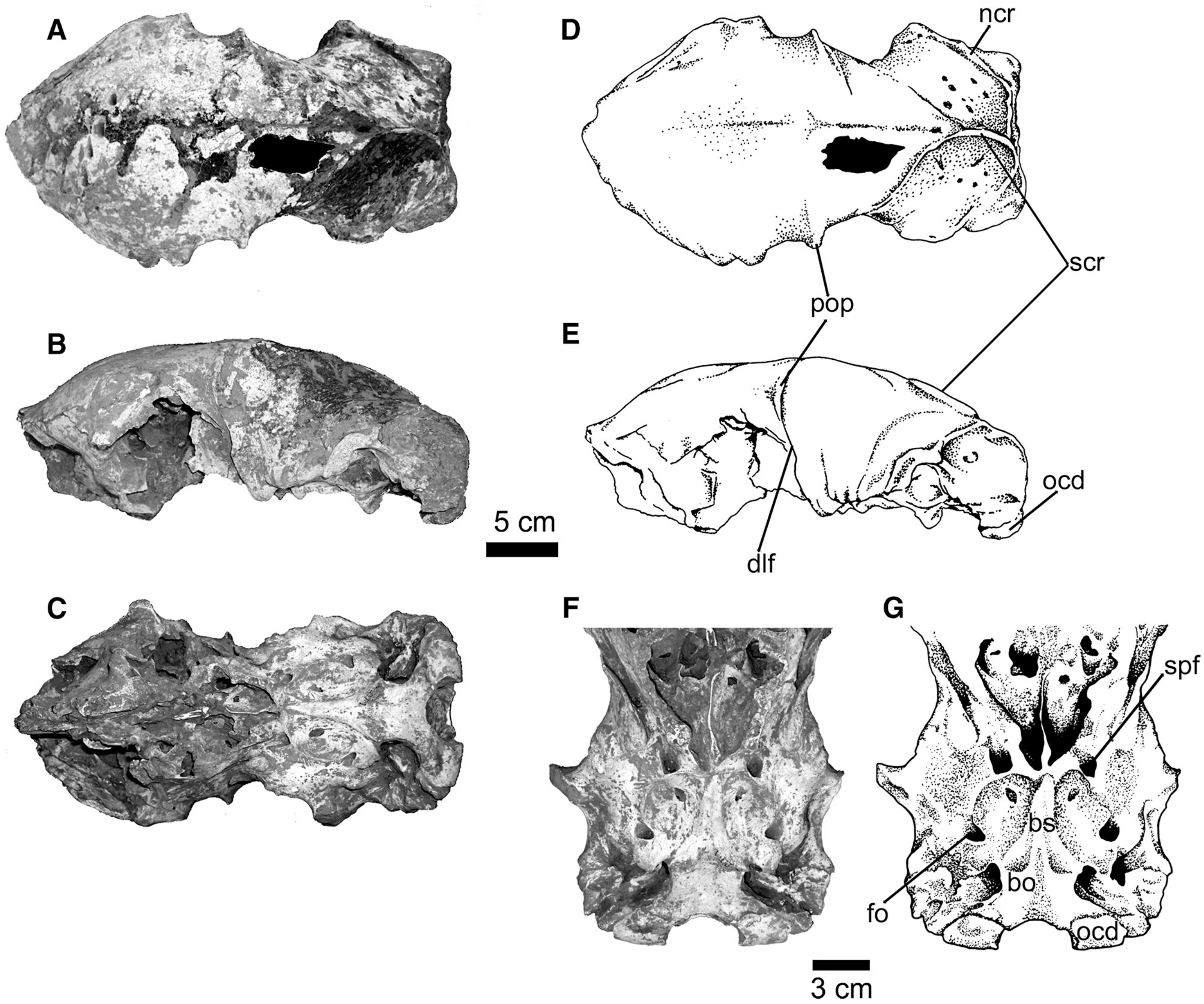

FIGURE 3. Skull of *Hoplophorus euphractus*. **A** and **D**, dorsal view; **B** and **E**, lateral view; **C**, ventral view. **F** and **G**, detail of the basicranium. **Abbreviations**: **bo**, basioccipital; **bs**, basisphenoid; **dlf**, descending lamina of frontal; **fo**, foramen ovale; **ncr**, nuchal crest; **ocd**, occipital condyles; **pop**, postorbital process; **scr**, sagittal crest; **spf**, sphenorbital fissure.

the caudal ring is composed by four rows—one anterior, two median, and one posterior—of different shape, size, and sculpture: the osteoderms from the anterior row are pentagonal, but their sculptural pattern is hardly discernible in the preserved specimen; the osteoderms from the median rows are roughly hexagonal and bear a large main figure and faintly delimited small peripheral figures; the posterior row is composed of the largest osteoderms, which show greatly enlarged main figures, as in *Panochthus* and *Neosclerocalyptus*, and small peripheral figures restricted to the their lateral and proximal borders.

Caudal Tube—The caudal tube (MHN 1005; Fig. 2E–H) has a conical-cylindrical shape with a nearly circular anterior end and a posteriorly decreasing dorsoventral height. Its size is intermediate between *Panochthus* and *Neosclerocalyptus.* The anteriormost end comprises an immobile ring formed by three fused transverse rows of osteoderms. The dorsal side (Fig. 3E) shows nearly circular osteoderms with centrally positioned, flat to moderately excavated, subcircular main figures similar to those of the dorsal region of carapace, and 11–12 polygonal peripheral figures that are shared by adjacent osteoderms. The osteoderms from the ventral side (Fig. 3F) have larger, elliptical main figures with an anteroposterior major axis, except the anterior-most osteoderms, which have more circular figures. The lateral sides show osteoderms with large elliptical main figures with an anteroposterior major axis, larger than those of the osteoderms on the ventral side. The caudal tube is remarkable in having a single pair of lateral figures, unlike all known hoplophorines except some species of *Urotherium*. Unlike most hoplophorines*,* the terminal and lateral figures bear conspicuous, centrally positioned conical tubercles, strikingly similar to those observed in the lateral and terminal figures of *Neuryurus* and *Panochthus* (Fig. 3G). As in this latter genus, these figures have conspicuous crest-like margins. As in Panochthini (Castellanos, 1941), the lateral figures are proportionally larger than in other known hoplophorines (e.g., *Neosclerocalyptus*, *Stromaphorus*) and their dorsoventral diameter nearly matches the dorsoventral diameter of the caudal tube in its corresponding position. The surfaces of the lateral and terminal figures are pathologically affected, but they seem less striated than in *Panochthus* and *Neuryurus.* A punctuated texture, smoother than in *Panochthus,* was also reported and figured by Winge (1915:pl. XVI) in reference to caudal tube fragments collected by Lund, which are not pathologically affected. The lateral figures are separated from the terminal ones by a wider area than in all known hoplophorines (except *Panochthus*). As in *Panochthus,* the opposite terminal figures are separate at the dorsal side by a wide area, unlike *Neosclerocalyptus* and all other known hoplophorines, in which they almost contact each other. This area is occupied by two pairs of enlarged circular figures (Fig. 3H), one anterior and other posterior, somewhat similar to the apical figures observed in *Panochthus* (Castellanos, 1941).

Skull—The maxillary and palatal portions of the skull are badly damaged and both zygomatic arches are wanting (Fig. 3). The suture among the bones of the rostral region and brain case are not visible, indicating that the skull probably belonged to an old individual. The rostrum as a whole is transversally expanded, as noted by Winge (1915) and Paula Couto (1957), more than in *Panochthus* and *Glyptodon*, but less than in *Neosclerocalyptus*. It narrows anteriorly in dorsal view and does not present the strongly developed pneumatized fronto-nasal sinuses observed in *Neosclerocalyptus* (Zurita et al., 2005). Unlike *Neosclerocalyptus,* the fronto-nasal area is slightly convex in lateral view and inclines anteriorly, though less than in *Panochthus*, making the skull very convex dorsally in lateral view. This feature is more visible in the anterior skull fragment figured by Winge (1915:pl. 17, Fig. 2), which includes a better-preserved rostrum. The postorbital process is well developed, anteroposteriorly compressed, and extended ventrally to form the descending lamina of the frontal. As in *Panochthus*, the occipital portion of the skull is not elevated relative to the rostral area in lateral view, unlike some species of *Neosclerocalyptus* (e.g., *N. ornatus*) and *Glyptodon*. The sagittal crest is relatively shorter but more marked than in *Neosclerocalyptus* and much shorter than in *Glyptodon.* The nuchal crest is marked and extends anteroventrally, reaching the ventrolateral third of the skull. The supraoccipital region is dorsoventrally short and anteriorly inclined, forming an angle of nearly 65° with the anteroposterior plane of the skull. The external occipital crest on the supraoccipital is less marked and sharper than in *Neosclerocalyptus*. On either side of this crest lies a noticeable fossa for attachment of the epaxial musculature, which is much wider than in *Neosclerocalyptus.* The foramen magnum is nearly circular, wider than high; its mediolateral width is nearly 30% the width of the occiput. The occipital condyles are roughly triangular, with long axes oriented mediolaterally as in *Glyptodon* rather than dorsoventrally as in *Panochthus*; *Neosclerocalyptus* presents both conditions. They project ventrally as in *Neosclerocalyptus* rather than caudally as in *Glyptodon* and *Panochthus*. The mastoid process projects less than in *Neosclerocalyptus*. The basicranium is the best-preserved portion of the skull (Fig. 3F–G). The basioccipital is Y-shaped, with branches diverging posteriorly to contact the occipital condyles; its surface is moderately concave. The basisphenoid is an elongate triangle with its apex pointing anteriorly and a strongly convex surface. At each side of the basisphenoid there are two pronounced oblong fossae with sharp lateral margins. Just anterior to each is a conspicuous sphenorbital fissure. In his original description of this material, Paula Couto (1957) confused this fissure with the foramen ovale, which lies more posteriorly. Anterolteral to the sphenorbital fissure, inside the well-marked groove formed by the medial side of the descending lamina of the frontal, lies the optic foramen. The foramen ovale opens posteriorly relative to the posterior root of the zygomatic arch, as in *Panochthus*, *Neosclerocalyptus*, and *Glyptodon*, slightly anterior to the contact between the basioccipital and the basisphenoid. The hypoglossal foramina are positioned on the lateral side of the posterior-most portion of each basioccipital branch, just anterior to the occipital condyles. As in *Neosclerocalyptus* and *Panochthus,* they are diminutive as compared to *Glyptodon*.

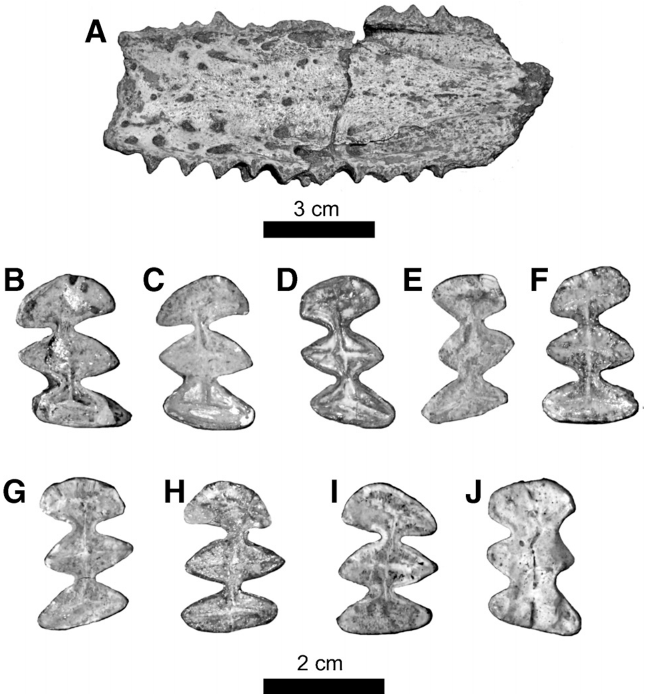

FIGURE 4. Palate and teeth of *Hoplophorus euphractus*. **A**, hard palate fragment MHN 755 in ventral view; **B–J**, upper molariforms from left to right, top to bottom: MHN 993, 994, 995, 996, 997, 998, 999, 1000, 1001.

Specimen MHN 755 (Fig. 4A) corresponds to the anterior and largest portion of the hard palate, which is formed by the palatine processes of the maxillae. The ventral surface medial to the toothrow is marked by several foramina of different sizes, more numerous than in *Neosclerocalyptus*. Anteriorly, at the level of the alveolus of the second molariform, one pair of foramina is much larger than the others and has pronounced sulci extending anteromedially that delimit a median triangular ventrally projected area.

Teeth—We were only able to locate 9 of the 10 isolated teeth originally described by Paula Couto (1957) (Fig. 4B–J). They are typically trilobate and present a ridge of osteodentine along the main axis of their occlusal surface, whith ramifications to each lobe. As in *Neosclerocalyptus*, there is no trace of additional smaller osteodentine ramifications similar to those observed in *Glyptodon* or *Panochthus* (Fernicola, 2008). In all teeth, the median lobe is oblong and all lobes have major axes oriented buccolingually. As acknowledged by Paula Couto (1957), the identification of isolated teeth is very complicated, as teeth from distinct loci are striking similar. All teeth are morphologically closer to the upper teeth of *Neosclerocalyptus* and *Panochthus*, which present a more triangular mesial lobe. MHN 993, 994, and 997 resemble left M6–8 and MHN 999, 1000, resemble right M6–8. MHN 995 and 1001 (left) and MHN 996 and 998 (right), are similar to M4–5 in having the mesial lobe more obliquely oriented and more lingually projected.

Scapula—Both scapulae, MHN 984 (Fig. 5A, B) and 985, lack the dorsal border. The scapular spine is well developed proximally. The infraspinous fossa is wider than the supraspinous fossa. As in *Neosclerocalyptus* and *Panochthus*, the caudal border of the scapula forms an angle of less than 60° with the dorsoventral axis of the scapular spine, unlike *Glyptodon* in which this

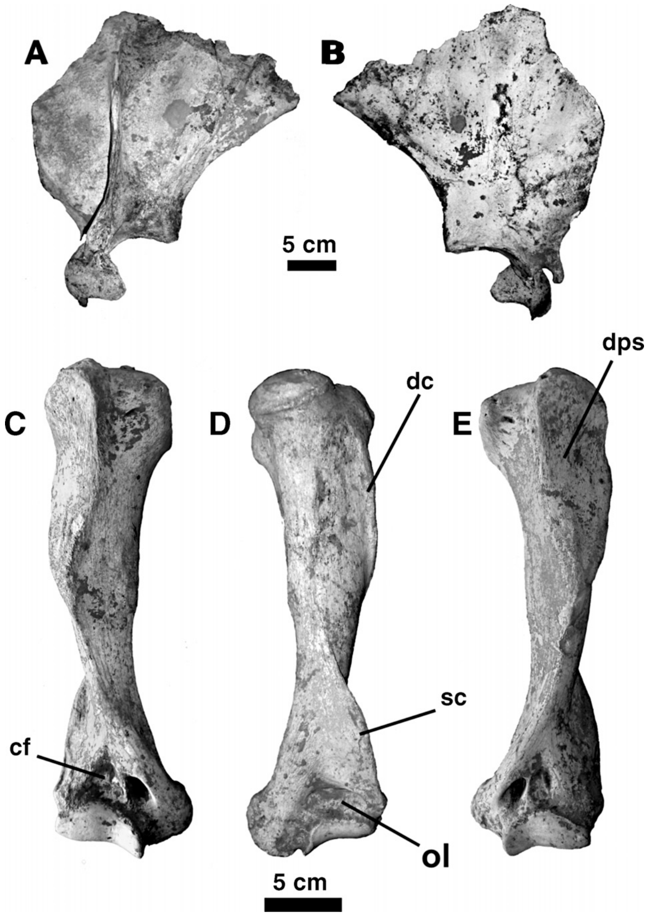

FIGURE 5. Forelimb elements of *Hoplophorus euphractus.* **A**, left scapula MHN 984 in lateral view; **B**, MHN 984 in medial view; **C**, right humerus MHN 987 in cranial view; **D**, right humerus MHN 987 in caudal view; **E**, left humerus MHN 986 in cranial view. **Abbreviations**: **cf**, coronoid fossa; **dc**, deltoid crest; **dps**, deltopectoral shelf; **ol**, olecranon fossa; **sc**, supinator crest.

angle is nearly 90°. The acromion process is well developed, roughly triangular, and has a convex surface. Its anterodistal border projects more ventrally than the posteroventral one and curves strongly medially as in *Neosclerocalyptus*, but does not form an elongated apophysis. The coracoid process does not hook medially as in *Neosclerocalyptus*. The glenoid fossa is nearly ovoid, with the cranial width nearly one and half times the caudal width, differing from both *Panochthus* and *Neosclerocalyptus*, in which the cranial width is nearly twice the caudal width.

Humerus—As in *Panochthus*, the humerus of *Hoplophorus* (Fig. 5C–E) is more slender than in *Neosclerocalyptus* and much more so than in *Glyptodon*. It is larger than the comparable element of *Neosclerocalyptus* but smaller than that of *Glyptodon* and *Panochthus*. As in more primitive glyptodonts (e.g., *Propalaehoplophorus*), the head is more elongated craniocaudally than in *Glyptodon*, *Neosclerocalyptus*, and *Panochthus*, in which it is more rounded. Its neck is poorly marked as in these genera. The bicipital groove is wider than in *Glyptodon*, *Neosclerocalyptus*, and *Panochthus.* The deltopectoral shelf has an elongated triangular shape as in *Panochthus* and ends near midshaft; it comprises nearly 50% of the humeral length, which is less than in *Neosclerocalyptus* (60%) but more than in *Glyptodon* (40%). It narrows to a point distally much more markedly than in *Neosclerocalyptus*, more like *Panochthus*. As in *Panochthus*, the deltoid and pectoral crests are less marked than in *Neosclerocalyptus*. The medial epicondyle is as developed as in *Panochthus* and *Neosclerocalyptus*, but much less robust than in *Glyptodon*. The shape and development of the lateral epicondyle is almost identical to that observed in *Neosclerocalyptus* and *Panochthus*. Like *Panochthus* and *Glyptodon*, the supinator crest starts distal to midshaft instead of at midshaf as in *Neosclerocalyptus*; it is slightly more laterally expanded than in *Panochthus* and *Neosclerocalyptus* and much more than in *Glyptodon*. The coronoid fossa has a nearly triangular shape. The olecranon fossa is deep. As in *Panochthus* and *Neosclerocalyptus* and unlike *Glyptodon*, a supracondyloid foramen is present. The bone bridge above this foramen is somewhat wider than in *Neosclerocalyptus.*

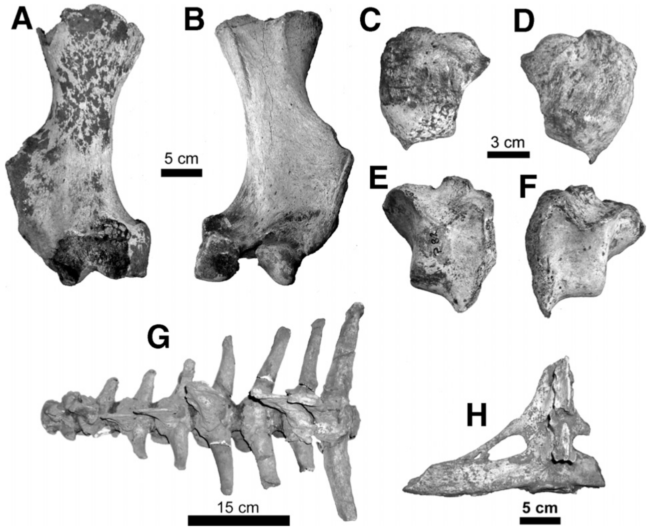

FIGURE 6. Hind limb elements, sacrum, and caudal vertebrae of *Hoplophorus euphractus.* **A**, right femur 988 in cranial view; **B**, right femur in caudal view; **C**, right patella MHN 990 in cranial view; **D**, left patella MHN 989 in cranial view; **E**, right patella MHN 990 in caudal view; **F**, left patella MHN 989 in caudal view; **G**, caudal vertebrae MHN 1006 in dorsal view; **H**, sacrum MHN 991 in dorsal view.

Femur—Only the distal half of a right femur (MHN 998; Fig. 6A–B) is preserved in the material collected in Lapa do Borges. The preserved portion is more slender than in *N. ornatus.* The supratrochlear fossa is deep and triangular as in *Panochthus* and *Neosclerocalyptus*, unlike *Glyptodon* in which it is more rounded. The medial condyle is larger and projects more distally than the lateral; in distal view, its articular surface is triangular with its cranial apex curved medially, and is roughly rounded in caudal view, where it is more developed than in *N. ornatu*s, as in *Glyptodon.* The lateral condyle is roughly triangular and proportionally more robust than in *N. ornatus* and *Panochthus*. The intercondyloid fossa is wider cranially than caudally, where it is deeper.

Patella—The patella of *H. euphractus* (MHN 989, 990; Fig. 6C–F) is roughly triangular and robust as in large Pleistocene glyptodonts (e.g., *Panochthus, Glyptodon*). As in *Glyptodon* and primitive glyptodonts (e.g., *Propalaehoplophorus*), its medial and lateral proximal borders are symmetrically developed, unlike in *Panochthus* and *Neosclerocalyptus* in which the lateral border is much more developed and proximally projected than the medial. The medial-most border of the proximal half forms a sharp projection, differing from *Panochthus* and *Glyptodon* in which it is more rounded. The distal-most portion of the lateral side forms a conical sharp projection that is not observed in *Panochthus*, *Neosclerocalyptus*, or *Glyptodon.* The articular facets for the patellar trochlea are separated by a well-developed median crest.

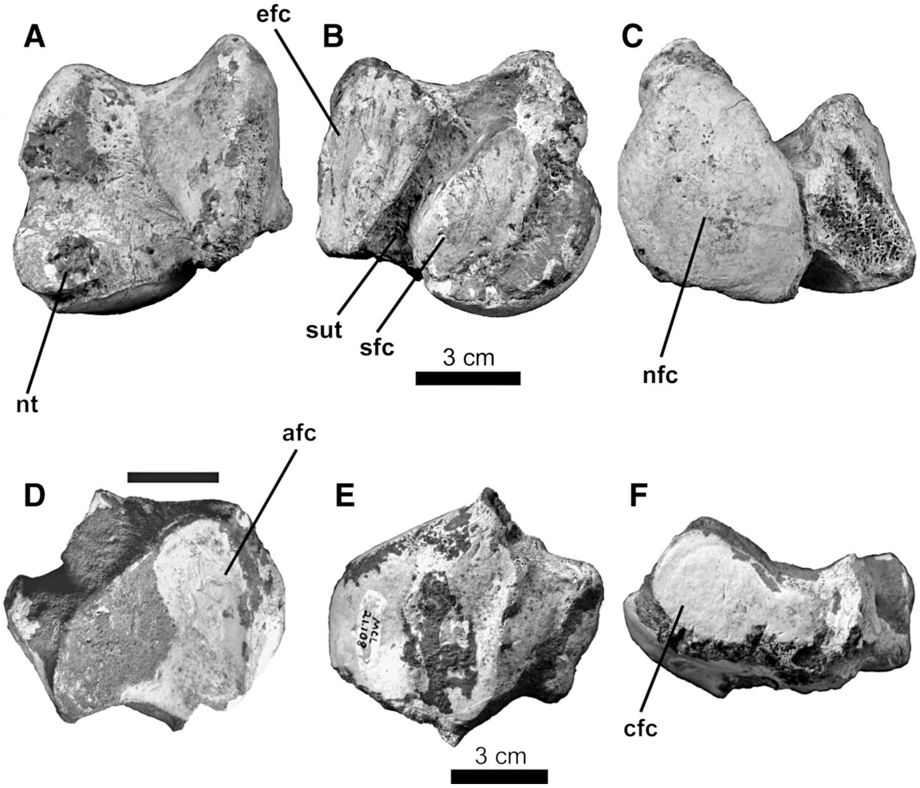

FIGURE 7. Tarsal elements of *Hoplophorus euphractus*. **A**, left astragalus MCL 21.107 in cranial view; **B**, left astragalus MCL 21.107 in caudal view; **C**, left astragalus MCL 21.107 in distal view; **D**, left navicular MCL 21.108 in proximal view; **E**, left navicular MHN 21.108 in distal view; **F**, left navicular MCL 21.108 in lateral view. **Abbreviations**: **afc**, astragalar facet; **cfc**, cuboid facet; **ecf**, ectal facet; **nfc**, navicular facet; **nt**, navicular tuberosity; **sfc**, sustentacular facet; **sut**, sulcus tali.

The lateral facet is proximally concave along its mediolateral axis and distally convex; its distal-most part curves dorsally, forming a right angle with the rest of the facet. The medial facet is concave along its proximodistal axis and forms an angle of almost 90° with the lateral one.

Astragalus—The astragalus of *H. euphractus* (MCL 21.107; Fig. 7A–C) is close in overall morphology to the comparable elements of *Panochthus* and *Neosclerocalyptus*. The trochlea is strongly asymmetrical due to the grater development of its lateral crest, which unlike in *Glyptodon* is more proximally projected than the lateral one; it is slightly less projected than the lateral one in *Panochthus* and *Neosclerocalyptus*. The groove between the crests of the astragalar trochlea is as wide and deep as in *Panochthus* and *Neosclerocalyptus* and deeper and wider than in *Glyptodon*. The ectal facet is nearly flat and is triangular as in *Panochthus* and *Neosclerocalyptus*, though somewhat more proximodistally elongated. As in *Glyptodon*, the sustentacular facet is oblong and more proximodistally elongated than in *Panochthus* and *Neosclerocalyptus*. It is nearly as long as the ectal, as in *Glyptodon*, unlike both *Panochthus* and *Neosclerocalyptus* in which it is much shorter than the ectal. The sulcus tali is deeper and wider than in *Neosclerocalyptus* and *Glyptodon*, more like *Panochthus*. The tuberosity for the medial collateral ligament is as developed as in *Panochthus* and *Neosclerocalyptus* but less than in *Glyptodon*. The facet for the navicular is roughly triangular with rounded edges as in *Panochthus*, *Neosclerocalyptus*, and *Glyptodon.* A navicular tuberosity occurs just proximal to the dorsal border of the navicular facet; it is quite flat proximodistally as in *Panochthus* and *Neosclerocalyptus* rather than cylindrical as in *Glyptodon*.

Navicular—The left navicular (MCL 21.108; Fig. 7D–F) is strongly proximodistally compressed as in *Glyptodon*, *Panochthus*, and *Neosclerocalyptus*. The articular facet for the astragalus is triangular, as in *Glyptodon*, *Panochthus*, and *Neosclerocalyptus*, but shows a more elongated outline than in these genera. The cuboid facet, which occupies most of the lateral surface, is ovoid and, as in *Glyptodon* and *Panochthus*, it is more mediolaterally elongated than in *Neosclerocalyptus*. At the distal side, the facet for the lateral cuneiform is roughly triangular as in *Neosclerocalyptus* and *Panochthus* but unlike *Neosclerocalyptus*, it does not contact dorsally the facet for the intermediate cuneiform. The facet for the intermediate cuneiform is oblong as in *Panochthus*, *Neosclerocalyptus*, and *Glyptodon* with its major axis oriented dorsoplantarly. The lateral-most plantar process is lacking; the medial-most is slightly less developed than in *Neosclerocalyptus* and *Panochthus*.

Sacrum and Caudal Vertebrae—The fragment of sacrum (MHN 991; Fig 6H) corresponds to the two caudal-most vertebrae strongly fused by their centra. The transverse processes of the penultimate vertebra are weakly developed and fused with the strongly developed processes of the last vertebra at each side, as in *Panochthus* and *Neosclerocalyptus*, delimiting the ovoid caudal-most sacral foramen. A sequence of eight caudal vertebrae is preserved (MHN 1006; Fig. 6G). As in *Glyptodon* and *Panochthus*, the hemal arches of the proximal-most vertebrae are more dorsoventrally elongated than in the distal-most ones, where they become shortened and more expanded craniocaudally. As in *Panochthus* and *Neosclerocalyptus*, the transverse processes are narrower than in *Glyptodon*.

DISCUSSION

When Paula Couto (1957) diagnosed *Hoplophorus*, he concentrated on cranial and exoskeletal characters (e.g., more elongated and narrower skull, less developed fronto-nasal sinuses, a single pair of lateral figures in the caudal tube, and more rounded dorsal carapace osteoderms) in order to differentiate this genus from *Neosclerocalyptus*. Regarding the postcranium, he mentioned only the presence of a more slender humerus and femur in *Hoplophorus*. Our comparative description revealed several additional postcranial and cranial differences between *Hoplophorus* and *Neosclerocalyptus* that reinforce the validity of the Brazilian genus: shorter sagittal crest, deeper fossae on either side of external occipital crest, less marked deltoid crest of humerus, astragalus with wider sulcus tali and more proximodistally elongated sustentacular facet, navicular with larger cuboid facet, and facets for the lateral and intermediate cuneiforms not contacting dorsally. Moreover, the partial carapace shows a much less elongated outline and a more convex dorsal profile relative to *Neosclerocalyptus*. On the other hand, *Hoplophorus* shares several similarities with *Panochthus* that are not shared with *Neosclerocalyptus*, such as a more ventrally inclined nasal area and a caudal tube with tubercle-like projections in the lateral and terminal figures, as noted by previous authors (Winge, 1915; Hoffstetter, 1958). Additional unreported similarities include the broad humerus, deep sulcus tali of the astragalus, more mediolaterally elongated cuboid facet of navicular, and caudal tube with large lateral figures separated from the terminal ones by wide spaces.

Hoplophorus was included in Hoplophorinae by Paula Couto (1947, 1957) but he failed to give explicit reasons to support his decision. In fact, *Hoplophorus* shares several cranial, postcranial and exoskeletal characters with the better-known genera included in this subfamily (e.g., *Panochthus* and *Neosclerocalyptus*, as discussed above). However, despite its wide acceptance (Simpson, 1945; Hoffstetter, 1958; McKenna and Bell, 1997), this group has been poorly diagnosed and has no clear synapomorphies. Hoffstetter (1958) recognized Hoplophorinae as a large assembly of glyptodonts sharing a greater specialization of teeth, skull, and limb bones (as compared to the propalaehoplophorines), absence of manual and pedal digit I, and possession of a conical-cylindrical caudal tube. Cattoi (1966) added to this list the presence of an anteriorly angled ascending ramus of the dentary and absence of smaller secondary ramifications of osteodentine in molariforms. Nonetheless, these characters are hardly diagnostic, as they are also shared with non-hoplophorine glyptodonts. *Doedicurus* (Doedicurinae) and *Glyptodon* (Glyptodontinae) are equally or more specialized than most of Hoplophorinae relative to the Propalaehoplophoridae (sensu Fernicola, 2008); they both lack manual digit I and have an anteriorly angled ascending ramus of the dentary, and *Doedicurus* has a tetradactyl pes (Ameghino, 1889; Lydekker, 1894; Paula Couto, 1979). In addition, *Glyptodon* bears strongly shortened metatarsals and lacks the supracondyloid foramen (Burmeister, 1870–74; Cattoi, 1966) which are clearly derived conditions compared to the elongated metatarsals and developed supracondyloid foramen present in both Hoplophorinae and Propalaehoplophoridae (Paula Couto, 1979). The presence of secondary ramifications of osteodentine are reported for the molariforms of *Glyptodon* (Burmeister, 1874) and *Doedicurus* (Fernicola, 2008), but also for hoplophorine glyptodonts (*Panochthus*; Fernicola, 2008). Finally, a conical-cylindrical caudal tube is also observed in *Eleutherocercus* (Doedicurinae), which, like most hoplophorines, also bears enlarged lateral figures diminishing in size from its distal extremity (Castellanos, 1940). These considerations are reinforced by the cladistic analysis of glyptodonts carried out by Fernicola (2008); no support was found for a monophyletic Hoplophorinae, though *Hoplophorus* itself was not included in the data matrix, which was based solely on craniomandibular characters.

Based mostly on character variation in the carapace and caudal tube, Hoffstetter (1958) tentatively subdivided Hoplophorinae into seven tribes (Paleohoplophorini, Plohophorini, Panochthini, Lomaphorini, Neothoracophorini, Neuryurini, and Hoplophorini) and placed *Hoplophorus*, together with *Neosclerocalyptus* and several late Miocene to Pliocene genera (e.g., *Hoplophractus, Eosclerocalyptus*), in the tribe Hoplophorini. This arrangement has been followed unchanged (Paula Couto, 1979) or with slight modifications (McKenna and Bell, 1997) in latter influential systematic works. Nonetheless, there are two main reasons that lead us to doubt the reliability of this arrangement. First, the naturalness of Hoplophorini seems unconvincing, as the diagnostic characters Hoffstetter (1958) proposed for this group, based mostly on the type genus "*Sclerocalyptus*" (= *Neosclerocalyptus* sensu Paula Couto, 1957), have a wider distribution within Glyptodontidae, being present in other hoplophorine tribes (e.g., development of the fronto-nasal sinuses, present in Panochthini) or even in non-hoplophorine glyptodonts (e.g., osteoderm with rosette pattern, present in most Hoplophorinae as well as in *Propalaehoplophorus* [Propalaehoplophorinae] and *Glyptodon* [Glyptodontinae]). Second, *Hoplophorus* differs from all purported Hoplophorini (sensu Hoffstetter, 1958) in having highly distinctive caudal tube characters, including a single pair of lateral figure, as in some species assigned to *Urotherium* (Lomaphorini; Castellanos, 1926) and *Doedicurus* (Doedicurinae; Castellanos, 1940), as well as in having strong centrally positioned tubercle-like projections in both lateral and terminal figures of the caudal tube, a character reported so far only for Panochthini (Castellanos, 1941) and *Neuryurus* (Neuryurini; Ameghino, 1889).

Phylogenetic Analysis

To evaluate the phylogenetic relationships of *Hoplophorus* within Glyptodontia (sensu Fernicola, 2008), we performed a cladistic analysis of 18 taxa scored for 151 morphological characters (Appendix 3). The characters include 84 craniodental characters from Fernicola (2008), of which 3 were originally proposed by Gaudin and Wible (2006), and 67 postcranial characters, 46 of which are from a work by the authors on the analysis of new *Pachyarmatherium* remains from northeastern Brazil (Porpino et al., 2009) and 21 of which are new (see Appendix 2 for descriptions and sources of each character). Postcranial characters were derived and scored via direct observation of specimens and from descriptions and figures in the literature (see Appendix 1). Forty-four multistate characters were treated as ordered in the analysis based on numerical and structural morphoclines following the 'method of intermediates' (Wilkinson, 1992). All characters were weighted equally. The ingroup incorporates all glyptodonts originally employed by Fernicola (2008) plus *Hoplophorus*. The Hoplophorinae (sensu Hoffstetter, 1958) are represented by eight well-known genera representing five of the seven tribes proposed by Hoffstetter (1958): *Panochthus* (Panochthini), *Plohophorus*, *Pseudoplohophorus*, *Stromaphorus* (Plohophorini), *Urotherium* (Lomaphorini) *Neosclerocalyptus*, *Hoplophorus*, *Hoplophractus*, and *Eosclerocalyptus* (Hoplophorini). Perea (2005; see also Zurita and Aramayo, 2007) considered *Hoplophractus* as a junior synonym of *Eosclerocalyptus* based on a multivariate analysis and argued that the cranial (e.g., the height of the choanae) and carapace characters traditionally used to separate the former from the latter would support specific rather than generic separation. Fernicola (2008), however, noted that the height of choanae, as well as other characters not mentioned by Perea (2005) (e.g., number of trilobed upper molariforms), are constant in the remaining glyptodonts and therefore a generic separation seems valid, at least for the species here considered to represent *Hoplophractus* (*H. tapinocephalus*) and *Eosclerocalyptus* (*E. planus*). Three tribes assigned to Hoplophorinae (Hosffstetter, 1958; McKenna and Bell, 1997), Neuryurini, Neothoracophorini, and Palaehoplophorini, were not included because they are poorly known. Other included glyptodonts represent three of the other four subfamilies recognized by Hoffstetter (1958): Propalaehoplophorinae (*Propalaehoplophorus, Eucinepeltus*), Doedicurinae (*Doedicurus*), and Glyptodontinae (*Glyptodon*). Skull and postcrania of Glyptatelinae glyptodonts are almost unknown (Fernicola, 2008; Croft et al., 2007) and for that reason they were excluded from the present analysis. Following Fernicola (2008), we used as outgroups three dasypodids (*Eutatus*, *Dasypus*, and *Euphractus*), one Pampatheriidae (*Pampatherium*), plus the enigmatic genus *Pachyarmatherium* (Downing and White, 1995) based on recently reported material from northeastern Brazil (Porpino et al., 2009). We believe that this expanded matrix not only provides a test for the position of the *Hoplophorus* but also offers an opportunity to reevaluate the status of Hoplophorinae/Hoplophorini based on a more comprehensive data set. The data matrix was analyzed under the criterion of maximum parsimony, using the branch-and-bound algorithm of PAUP version 4.0b10* (Swofford, 2002). Variation within terminal taxa was treated using the 'Uncertain' option of PAUP, which does not take into account character state changes within terminals (Swofford, 1991). We report only unambiguous synapomorphies (i.e., those recovered under both ACCTRAN and DELTRAN optimizations). Clade support was accessed by calculating Bremer support (Bremer, 1994) and performing a bootstrap analysis (Felsenstein, 1985) with the same settings as the original analysis using the branch-and-bound algorithm and 1000 replicates.

The analysis resulted in a single most parsimonious tree (MPT) (tree length = 320, CI = 0.64, RI = 0.75; Fig. 8) and six characters were considered parsimony uninformative. Regarding the outgroups, *Pampatherium* is positioned as the sister group to glyptodonts, with *Pachyarmatherium* as the sister group to *Pampatherium* + Glyptodontia, echoing the findings of Porpino et al. (2009). The monophyly of Glyptodontia (sensu Fernicola, 2009; node A) is supported by 36 unambiguous synapomorphies and has good bootstrap and Bremer values (98 and 4, respectively). Of these 36 unambiguous synapomorphies, 29 were previously found by Fernicola (2008; 4:2, 6:1, 7:0, 9:1, 10:1, 15:2, 16:1, 19:0, 24:2, 26:1, 31: 2, 40:2, 42:1, 46:1, 48:1, 55:1, 57:1, 59:2, 61:1, 63:1, 65:2, 67:2, 68:2, 70:1, 72:2, 76:2, 79:1, 82:2, and 84:1) and 7 represent new postcranial characters: supinator crest of humerus moderately developed, comprising 60–70% of the width at the epicondyles (101); third trochanter of femur positioned bellow midshaft (109); robust tuber of calcaneum (120); fibular facet of calcaneum absent (124); presence of a navicular tuberosity in astragalus (130); flat to convex sustentacular facet of astragalus (137); and ectal facet of astragalus nearly triangular (140). Character states 4:2, 6:1, 9:1, 10:1, 15:2, 24:2, 40:2, 48:1, 55:1, 57:1, 59:2, 65:1, 67:2, 68:1, 72:2, 101:1, 109:1, 120:1, and 130:1 are synapomorphies unique to the node A. The Propalaehoplophoridae (sensu Fernicola, 2008; node B) are the sister group to the remaining glyptodonts (node C), which form a well-supported clade (bootstrap: 95%; Bremer = 6) diagnosed by seven unambiguous synapomorphies: last four lower molariforms trilobed, with triangular mesial lobe (21); foramen ovale posterior to the glenoid fossa (36); transverse foramen absent (37); glenoid fossa positioned by less than one molariform length posterior to the upper toothrow (65); occipital condyles higher than wide (81); angle between the occipital plane and the horizontal plane of the skull <65° but ≥45° (82); and caudal armor composed by proximal rings of osteoderms plus distal caudal tube (146). One of the main differences of the MPT obtained compared to the results of Fernicola (2008) is the stability of *Urotherium* as the sister group to the clade (*Plohophorus* (*Doedicurus* + *Glyptodon*)). However, this position is supported by a single unambiguous synapomorphy (lacrimal foramen ventrally positioned relative to the occipital condyle; 75) and has both low bootstrap and Bremer support values.

As in Fernicola (2008), our results strongly contradict the monophyly of Hoplophorinae (sensu Hoffstetter, 1958), indicating that it is paraphyletic assemblage of glyptodonts more derived than the Propalaehoplophoridae (sensu Fernicola, 2008) but outside the clade formed by *Glyptodon* + *Doedicurus.* Nonetheless, some subsets of taxa within this assemblage do form monophyletic groups (nodes H and I), though their contents do not match any of the tribes proposed by Hoffstetter (1958), Paula Couto (1979), or McKenna and Bell (1997). The Hoplophorini (sensu Hoffstetter, 1958; McKenna and Bell, 1997) is also clearly paraphyletic, as it corresponds to node C minus *Panochthus* and node L.

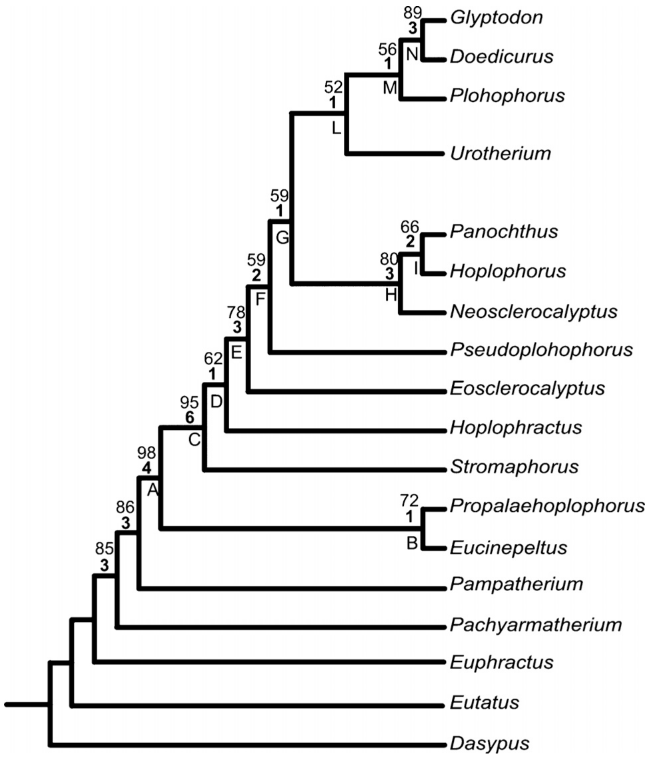

FIGURE 8. MPT of relationships of Glyptodontia including *Hoplophorus*. Capital letters indicate nodes discussed in the text; numbers above nodes are Bremer support values; bold numbers indicate bootstrap values. Tree length = 320; CI = 0.64; RI 0.75.

In the obtained topology, *Hoplophorus* is the sister group to *Panochthus* (node I). This alliance is supported by five unambiguous synapomorphies: the last seven or all maxillary molariforms trilobed (27); presence of conical tubercle in the lateral and terminal figures of caudal tube (147); length of L1 >90% of the length of terminal figure (149); terminal figures of caudal tube clearly separated dorsally (150); and dorsoventral diameter of L1 subequal to the dorsoventral diameter of the caudal tube at its corresponding position (151). This is an interesting result given that *Hoplophorus* was previously believed to be more closely allied to *Neosclerocalyptus* (Ameghino, 1889; Winge, 1915; Hoffstetter, 1958). *Neosclerocalyptus* is placed as the sister group to *Hoplophorus* + *Panochthus* in node H (Panochthidae sensu Fernicola, 2008), which is supported by 17 unambiguous synapomorphies (2:3, 29:2, 31:2, 45:1, 46:3, 53:1, 54:1, 55:2, 58:1, 73:1, 77:1, 85:1, 87:1, 116:1, 117:1, 129:1, and 131:1). This position is congruent with the stratigraphic evidence, as *Neosclerocalyptus* has the oldest record (Marplatan to late Lujanian; Zurita et al., 2005) within node H.

The phylogenetic perspective provided by our analysis helps to clarify the evolution of some of the most peculiar exoskeletal characters of *Hoplophorus*. The occurrence of a single pair of lateral figures (character 148) in *Hoplophorus* and *Doedicurus* was optimized in the MPT as independently acquired. Unlike *Hoplophorus*, the single pair of lateral figures in *Doedicurus* has a markedly depressed surface and does not show the striking conical tubercular projections seen in this latter genus. The presence of a single pair of lateral figure is reported for some species of *Urotherium* (*U. simplex*; Castellanos, 1926) but others (*U. simile*) present several less-developed large figures anterior to the largest distal one (Castellanos, 1948). Moreover, in *Urotherium* this figure differs from both *Hoplophorus* and *Doedicurus* in being smoother, and does not present either a concave surface (as in *Doedicurus*) or conical tubercles (as in *Hoplophorus*). The presence of a central conical tubercle in the lateral and terminal figures (character 147) was optimized in the MPT as a synapomorphy of node I. According, the morphology of the terminal and lateral figures in *Panochthus* (and other Panochthini; see Castellanos, 1941) and *Hoplophorus* is strikingly similar in having a proportionally greater dorsoventral diameter and marked crest-like edges compared to *Neosclerocalyptus*. The presence of conical tubercles in lateral and terminal figures also is shared with the poorly known genus *Neuryurus*, which was not included in our data matrix. In fact, this character led Lydekker (1897) to attribute a fragment of caudal tube from Minas Gerais state housed in collection of the British Museum to *Euryurus rudis* (= *Neuryurus rudis*). This specimen likely belongs to *H. euphractus* (Winge, 1915). Despite the shared presence of conical tubercles in the lateral and terminal figures, *Neuryurus* has highly distinctive exoskeletal characters, compared to both *Hoplophorus* and *Panochthus*; these include a caudal tube with quadrangular to polygonal poorly attached osteoderms with elevated main figures and carapace osteoderms with a raised central figure surrounded by well-developed foramina (Ameghino, 1889; Cattoi, 1966; Zurita et al., 2006) rather than a rosette pattern as seen in *Hoplophorus* and most glyptodonts, or the ornamental pattern observed in *Panochthus*, comprising small, randomly distributed figures (Burmeister, 1874; Castellanos, 1941). These differences make it difficult to establish the affinities of this genus and, consequently, to infer whether the presence of a conical tubercle in *Neuryurus* is homoplastic or homologous relative to *Hoplophorus* and *Panochthus*. In addition, the only cranial material attributed to this genus (Ameghino, 1889), which would provide valuable information on its affinities, was reassigned to *Urotherium* by Castellanos (1926).

Another remarkable caudal tube feature of *Hoplophorus* is the presence of two pairs of enlarged rounded figures in its posterior extremity, whose topographical position nearly corresponds to that of the apical and apex figures in *Panochthus* (Castellanos, 1941) and *Doedicurus* (Castellanos, 1940). In these latter genera, the apical figures are positioned posterior to the posterior-most dorsal figures and to a median posterior figure, a condition that facilitates their identification and recognition as putative homologous features. However, the absence of these morphological details in *Hoplophorus* render it difficult to evaluate whether the two pairs of rounded figures in the distal end of caudal tube of this genus are comparable to the structures recognized in *Panochthus* and *Doedicurus*.

The position of *Hoplophorus* in the MPT offers additional support for the validity of *Hoplophorus* as a genus distinct from *Neosclerocalyptus*, corroborating in a cladistic context the earlier hypothesis of Winge (1915) and Paula Couto (1947, 1957). It is not our purpose here to revise glyptodont systematics, as this work is being done elsewhere (see Fernicola, 2008). However, we advance here some suggestions regarding the classificatory scheme being proposed, hoping that it will contribute to its further refinement. Fernicola (2008) revalidated the subfamily Panochthinae originally proposed by Castellanos (1927) for the clade formed by *Neosclerocalyptus* and *Panochthus* and allocated these genera to the tribes Neosclerocalyptini and Panochthini, respectively. Based on the results of the present analysis, we propose the inclusion of *Hoplophorus* within Panochthinae (node I) in the tribe Hoplophorini as the sister group to Panochthini. In addition, we propose the allocation of *Neosclerocalyptus* to a new subfamily, Neosclerocalyptinae, as the sister group to Panochthinae

CONCLUSIONS

Our redescription of the material of *Hoplophorus euphractus* from Lapa do Borges, complemented by the description of additional specimens, allows a better differentiation between the genus *Hoplophorus* and its close allies, especially *Neosclerocalyptus*, in which it was originally included. Our cladistic analysis corroborates the monophyly of Glyptodontia (sensu Fernicola, 2008), presents new postcranial synapomorphies, and helps to improve its internal resolution, though bootstrap and Bremer support values for most internal nodes are still weak. Our results support the validity of *Hoplophorus* as a genus distinct from *Neosclerocalyptus* and place *Hoplophorus* as the sister group to *Panochthus* based on the presence of caudal tube synapomorphies. The topology obtained indicates that the subfamily Hoplophorinae (sensu Hoffstetter, 1958) is a large grade of all nonglyptodontine and doedicurine glyptodonts more derived than the propalaehoplophorines. Moreover, the diagnostic characters traditionally proposed for this subfamily are unsound, as they show a wider distribution within Glyptodontidae. Likewise, we find no support for the monophyly of the tribe Hoplophorini (sensu Hoffstetter, 1958). On the other hand, we propose here the redefinition of the tribe Hoplophorini in a restricted sense to name the lineage represented by *Hoplophorus*, making it the sister group of Panochthini within Panochthinae (sensu Fernicola, 2008). In addition, we propose a new subfamily, Neosclerocalyptinae, represented by *Neosclerocalyptus*, as the sister group to Panochthinae.

ACKNOWLEDGMENTS

We thank M. Reguero (MLP), C. Cardoso (MHN), M. F. C. F. Santos (MCC), A. Kramarz (MACN), C. Cartelle (MCL), M. Ubilla, D. Perea (FC-DPV), and S. M. Vaz (MNRJ) who kindly gave us access to the specimens under their care; R. G. G. Silva and L. H. B. Pereira for the drawings; and two anonymous reviewers for their comments and suggestions. This work was supported by Coordenação de Aperfeiçoamento de Pessoal de Nível Superior (CAPES).

LITERATURE CITED

Ameghino, F. 1889. Contribución al conocimiento de los mamíferos fósiles de la República Argentina. Actas de la Academia Nacional de Ciências de Córdoba 6:1–1027.

Ameghino, F. 1891. Mamíferos y aves fósiles argentinas. Especies nuevas adiciones y correcciones. Revista Argentina de Historia Natural 1:240–259.

Auler, A. S., L. B. Pilo, P. L. Smart, X. Wang, D. Hoffmann, D. A. Richards, R. L. Edwards, W. A. Neves, and H. Cheng. 2006. U-series dating and taphonomy of Quaternary vertebrates from Brazilian caves. Palaeogeography, Palaeoclimatology, Palaeoecology 240:508–522.

Bremer, K. 1994. Branch support and tree stability. Cladistics 10:295–304.

Burmeister, H. 1870–74. Monografia de los glyptodontes em el Museo Público de Buenos Aires. Anales del Museo Público de Buenos Aires 2:1–412.

Cabrera, A. 1944. Los gliptodontoideos del araucaniano de Catamarca. Revista del Museo de La Plata (Nueva Serie), Sección Paleontología 3:5–76.

Cartelle, C. 1999. Pleistocene mammals of the Cerrado and Caatinga of Brazil; pp. 27–46 in J. B. Eisenberg and K. H. Redford (eds.) Mammals of the Neotropics, Volume 3. Mammals of the Neotropics. University of Chicago Press, Chicago, Illinois.

Castellanos, A. 1926. Sobre un nuevo gliptodóntido chapadmalense, *Urotherium simplex* n. gen. et n. sp. y las formas afines. Anales del Museo Nacional de Historia Natural de Buenos Aires 34:263–278.

Castellanos, A. 1927. Descripción de un fragmento de tubo caudal de un doedicurino en relación con sus géneros afines. Anales del Museo de Historia Natural de Montevideo 2:265–300.

Castellanos, A. 1939. A propósito de los géneros *Plohophorus*, *Nopachthus* y *Panochthus* (1^a parte). Publicaciones del Instituto de Fisiografia y Geología 6:1–277.

Castellanos, A. 1940. A propósito de los géneros *Plohophorus*, *Nopachthus* y *Panochthus* (2^a parte). Publicaciones del Instituto de Fisiografia y Geología 8:280–414.

Castellanos, A. 1941. A propósito de los géneros *Plohophorus*, *Nopachthus* y *Panochthus* (3^a parte). Publicaciones del Instituto de Fisiografia y Geología, 11:417–592.

Castellanos, A. 1948. La presencia del genero "*Urotherium*" en el "Araucanense" del Valle de Yocavil (Santa Maria), provincias de Catamarca y Tucumán. Publicaciones del Instituto de Fisiografia y Geología 35:5–16.

Cattoi, N. V. 1966. Edentata; pp. 3–27 in A. V. Borello (ed.), Paleontografía Bonaerense, 4 Vertebrata. Comisión de Investigación Científica, Buenos Aires.

Croft, D. A., J. J. Flynn, and A. R. Wyss. 2007. A new basal glyptodontid and other Xenarthra of the early Miocene Chucal Fauna, northern Chile. Journal of Vertebrate Paleontology 27:781–797.

Downing, K. F., and R. S. White. 1995. The cingulates (Xenarthra) of the Leisey Shell Pit local fauna (Irvingtonian), Hillsborough County, Florida. Bulletin of Florida Museum of Natural History 37:375–396.

Felsenstein, J. 1985. Confidence limits on phylogenies: an approach using the bootstrap. Evolution 39:783–791.

Fernicola, J. C. 2008. Nuevos aportes para la sistemática de los Glyptodontia Ameghino 1889 (Mammalia, Xenarthra, Cingulata). Ameghiniana 45:553–574.

Gaudin, T. J., and J. R. Wible. 2006. The phylogeny of living and extinct armadillos (Mammalia, Xenarthra, Cingulata): a craniodental analysis; pp. 153–198 in M. T. Carrano, T. J. Gaudin, R. W. Blob, and J. R Wible (eds.), Amniote Paleobiology. Perspectives on the Evolution of Mammals, Birds and Reptiles. The University of Chicago Press, Chicago, Illinois.

Hill, R. V. 2006. Comparative anatomy and histology of xenarthran osteoderms. Journal of Morphology 267:1441–1460.

Hoffstetter, R. 1958. Xenarthra; pp. 535–636 in P. Piveteau (ed.), Traité de Paléontologie, Vol. 2, No. 6, Mammifères Évolution. Masson et cie, Paris.

Hoffstetter, R. 1964. Les Glyptodontes du Pléistocene de Tarija (Bolivie). I. Genres *Hoplophorus* et *Panochthus*. Bulletin de la Societé Geologique de France 7:126–133.

International Commission on Zoological Nomenclature (ICZN). 1999. International Code of Zoological Nomenclature. London, Internal Trust for Zoological Nomenclature, 306 pp.

Lund, P. W. 1839. Blik paa Brasiliens dyreverden för sidste jorgdomvaeltning. Anden afhandling: Pattedyrene (Lagoa Santa d. 16 de novbr. 1837). Det Kongelige Danske Videskabernes Selskabs Naturvidenskabelige og Mathematiske Afhandlinger 8:61–144.

Lund, P. W. 1840a. Blik paa Brasiliens dyreverden för sidste jorgdomvaeltning. Tredie afhandling: Fortsaettelse af Pattedyrene. Lagoa Santa d. 12te septbr. 1838). Det Kongelige Danske Videskabernes Selskabs Naturvidenskabelige og Mathematiske Afhandlinger 8:217–272.

Lund, P. W. 1840b. Tillaeg til de to sidste Afhandlinger over Brasiliens Dyreverden för Sidste Jordomvaeltning. Lagoa Santa, den 4de. April 1839. Det Kongelige Danske Videskabernes Selskabs Naturvidenskabelige og Mathematiske Afhandlinger 8:273–296.

Lund, P. W. 1842. Blik paa Brasiliens Dyreverden för Sidste orgdomvaeltning. Fjerde Afhandling: Fortsaettelse af Pattedyrene. Lagoa Santa den 30te. Januar 1841. Det Kongelige Danske Videskabernes Selskabs Naturvidenskabelige og Mathematiske Afhandlinger 9:137–208.

Lund, P. W. 1844. Conspectus Dasypodum. Oversigt over det Kongelige Danske Videnskabernes Selskabs Forhandlinger 1843:79–83.

Lund, P. W. 1846. Meddelelse af Det Udbytte de i 1844 undersögte knoglehuler Have afgivet til hundskaben om Brasiliens Dyreverden för Sidste Jordomvaetning. Lagoa Santa, d. 22de. November 1844. Det Kongelige Danske Videskabernes Selskabs Naturvidenskabelige og Mathematiske Afhandlinger 12:1–94.

Lydekker, R. 1894. Contributions to a knowledge of the fossil vertebrate of Argentina. Part 2. Extinct Edentates of Argentina. Anales del Museo de La Plata 3:1–118.

Lydekker, R. 1897. Catalogue of the fossil Mammalia in the British Museum. Part V. London, xxxvi + 346 pp.

McKenna, M. C., and S. K. Bell. 1997. Classification of Mammals above the species level. Columbia University Press, New York, 631 pp.

Neves, W. A., and L. B. Piló. 2003. Solving Lund's dilemma: new AMS dates confirm that humans and megafauna coexisted at Lagoa Santa. Current Research in the Pleistocene 20:57–60.

Owen, R. 1845. Descriptive and illustrated catalogue of the fossil organic remains of Mammalia and Aves contained in the Museum of the Royal College of Surgeons of London. R. and J. E. Taylor, London, 391 pp.

Paula Couto, C. 1947. Contribuição para o estudo de *Hoplophorus euphractus* Lund, 1839. Summa Brasiliensis Geologiae 1:1–14.

Paula Couto, C. 1957. Sôbre um gliptodonte do Brasil. Rio de Janeiro, Departamento Nacional de Produção Mineral, Divisão de Geologia e Mineralogia, 37 pp.

Paula Couto, C. 1979. Tratado de Paleomastozoologia. Rio de Janeiro, Academia Brasileira de Ciências, 590 pp.

Perea, D. 2005. *Pseudoplohophorus absolutus* n. sp. (Xenarthra, Glyptodontidae), variabilidad en Sclerocalyptinae y redefinición de una biozona del Mioceno Superior de Uruguay. Ameghiniana 42:175–190.

Piló, L. B. 1998. Morfologia cárstica e materiais constituintes: dinâmica e evolução da depressão poligonal Macacos-Baú-Carste de Lagoa Santa, MG. Ph.D. dissertation, Universidade Federal de Minas Gerais, 269 pp.

Porpino, K. O., J. C. Fernicola, and L. P. Bergqvist. 2009. A new cingulate (Mammalia: Xenarthra) *Pachyarmatherium brasiliense* sp. nov. from the late Pleistocene of northeastern Brazil. Journal of Vertebrate Paleontology 29:881–893.

Pouchet, G. 1866. Contribution a l'anatomie des édentés. Journal de L'anatomie et de la Physiologie 3:337–353.

Simpson, G. G. 1945. The principles of classification and a classification of mammals. Bulletin of the American Museum of Natural History 85:1–350.

Swofford, D. L. 1991. PAUP: Phylogenetic Analysis Using Parsimony, Version 3.1 Computer program distributed by the Illinois Natural History Survey, Champaign, Illinois.

Swofford, D. 2002. PAUP*. Phylogenetic Analysis Using Parsimony (*and Other Methods). Version 4.0 b10. Sinauer Associates, Sunderland, Massachusetts.

Wilkinson, M. 1992. Ordered versus unordered characters. Cladistics 8:375–385.

Winge, H. 1915. Jordfundne og nulevende Gumlere (Edentata) fra Lagoa Santa, Minas Gerais, Brasilien. Méd udsigt over gumlernes indbyrdes slaegtskab. E Museo Lundii 1:1–200.

Zurita, A. E., and S. A. Aramayo. 2007. New remains of *Eosclerocalyptus tapinocephalus* (Cabrera) (Mammalia, Xenarthra, Glyptodontidae): description and implications for its taxonomic status. Revista Italiana di Paleontologia e Stratigrafia 113:57–66.

Zurita, A., G. J. Scillato-Yané, and A. A. Carlini. 2005. Paleozoogeographic, biostratigraphic, and systematic aspects of the genus *Sclerocalyptus* Ameghino, 1891 (Xenarthra, Glyptodontidae) of Argentina. Journal of South American Earth Sciences 20:121–129.

Zurita, A. E., G. J. Scillato-Yané, and A. Mones. 2007. Aspectos nomenclaturales de la Familia Glyptodontidae (Mammalia, Xenarthra): el caso de *Sclerocalyptus* Ameghino, *Hoplophorus* Lund y la Tribu Sclerocalyptini. Ameghiniana 44:241–244.

Zurita, A. E., E. Soilbelzon, and A. A. Carlini. 2006. *Neuryurus* (Xenarthra, Glyptodontidae) in the Lujanian (late Pleistocene–early Holocene) of the Pampeam region. Neues Jahrbuch fur Geologie und Paleontologie Manatshefte 241:78–88.

Zurita, A. E., A. R. Miño-Boilini, E. Soibelzon, A. A. Carlini, and F. P. Ríos. 2009. The diversity of Glyptodontidae (Xenarthra, Cingulata) in the Tarija Valley (Bolivia): systematic, biostratigraphic and paleobiogeographic aspects of a particular assemblage. Neues Jahrbuch für Geologie und Paläontologie 251:225–237.

Submitted March 9, 2009; accepted September 29, 2009.

APPENDIX 1. Specimens examined and references consulted for comparative study and cladistic analysis.

Euphractus sexcinctus: MN 4975, 4979, 4988, 4990, 4991, 4993, 23981, 24013, 51654; MACN-Ma: 45.30, 50.121, 11.24, 20.3, 20.4, 14317, 34.592, 34.714, 47.204, 299

Dasypus novemcinctus: MN 1679, 4669, 4672, 5009, 6010, 51653; MACN-Ma: 49.391, 49.397, 49.350, 49.383, 50.123, 50.124, 39.461

Eutatus seguini: MLP 84-II-6-1, 69-VIII-22-4, 69-VIII-1-4, 69-VIII-1-5, 69-VIII-1-8; MACN-Pv 985, 1982, 10177

Eutatus sp.: MLP 16-146, 16-221, 00-VIII-51, 42-IX-1-2, 69-VIII-22-13

Pampatherium typum: MACN-Pv 11543/4, 11544, 11474, 11522; MLP-81-X-30-1; MHD-P-28

Pampatherium humboldti: MCL 900/01, 900/02, 900/03, 900/04, 900/05, 900/07, 900/08, 900/87

Pachyarmatherium: MCC 379-V, 423-V, 996-V, 759-V, 760-V, 761-V, 762-V, 769-V, 783-V, 994-V, 1133-V, 1134-V

Propalaehoplophorus australis: MLP 16-15

Propalaehoplophorus minus: MACN A-4757

Propalaehoplophorus sp.: MLP 91-II-25-6; MACN A-4754, A-7655, A-7656

Eucinepeltus petesatus: MACN A-4758 (holotype)

Eucinepeltus sp.: MLP-84-III-1-1

Eosclerocalyptus planus: MACN-Pv 4853; Cabrera (1944)

Neosclerocalyptus sp.: MACN-Pv 8773, 15151, 18107; MLP 16-28; Zurita et al. (2005)

Hoplophorus euphractus: studied material (see text); Winge (1915)

Hoplophractus tapinocephalus: MLP-37-III-7-7 (Holotype); Cabrera (1944), Zurita and Lutz (2007)

Panochthus intermedius: MLP 16—37; Castellanos (1941)

Panochthus tuberculatus: MLP 16-29; Burmeister (1871-74), Castellanos (1941)

Panochthus sp.: MACN 5130, 14998; MLP P-1 (old catalogue number), MLP MLP 16-38; Burmeister (1871-74)

Plohophorus figuratus: MLP 16-153 (holotype); Castellanos (1939)

Stromaphorus compressidens: MLP-29-X-8-1; Cabrera (1944)

Pseudoplohophorus absolutus: FC-DPV-475 and -595 (holotype)

Urotherium antiquus: MACN A-229-A-231

Glyptodon sp.: MACN 4, 17566, 10153, 1780

Glyptodon reticulatus: MACN 10153 and 1780

Glyptodon munizi: MACN-8706.

Doedicurus sp.: MLP 00-I-25-1 and 16-24; MACN 12572, 16295 15153, 2757, 2762; Castellanos (1940)

APPENDIX 2. List of characters and character states used in the cladistic analysis. Characters marked with an asterisk (*) are ordered. Characters modified from the original source are indicated. Abbreviations: LLM, last lower molariform; LUM, last upper molariform; L1, distal-most lateral figure of caudal tube.

(1) *Length of the anterior-most toothless portion of mandible: ≥25% of the total length of mandible (0); <25%, ≥10% of the total length of mandible (1); <10% of the total length of the mandible (2). (Modified from Fernicola, 2008, character 0).

(2) *Distance from the posterior border of the mandible to the anterior border of the last lower molariform measured as LLM length: ≥10 LLM length (0); <10, ≥3.5 LLM length (1); <3.5, ≥2.5 LLM length (2); <2.5 LLM length (3). (Modified from Fernicola, 2008, character 1).

(3) *Number of lower teeth hidden by the ascending ramus of mandible: zero (0); one (1); two (2); three (3). (Fernicola, 2008, character 2).

(4) *Distance between the condyloid process of the mandible and the posterior border of lower toothrow measured as LLM length: ≥10 LLM length (0); <10, ≥2 LLM length (1); <2 LLM length (2). (Modified from Fernicola, 2008, character 3).

(5) Position of the posterior border of the intermandibular symphysis relative to the first lower molariform: anterior (0); posterior (1). (Fernicola, 2008, character 4).

(6) Angle between the mandibular body and the ascending ramus: <90° (0); ≥90° (1). (Modified from Fernicola, 2008, character 5).

(7) Distinct lateral ridge of the coronoid process: absent (0); present (1). (Modified from Gaudin and Wible, 2006, character 21).

(8) *Position of the condylar process relative to coronoid and angular processes: condylar closer to the angular (0); condylar equidistant (1); condylar closer to the coronoid (2). (Modified from Gaudin and Wible, 2006, character 22).

(9) Relative position between the posterior-most border of the mandible and the condylar process: < width of the condylar process (0); ≥ width of the condylar process (1). (Modified from Fernicola, 2008, character 8).

(10) Shape of the posterodorsal portion of the angular process: strongly concave, hooks posteriorly (0); gently concave to convex (1). (Modified from Fernicola, 2008, character 9).

(11) *Depth of mandible: shallow, maximum depth of the horizontal ramus <10% of the maximum mandibular length (0); moderate, maximum depth of the horizontal ramus ≥10%, <20% of the maximum mandibular length (1); deep, maximum depth of the horizontal ramus ≥20% of the maximum mandibular length (2). (Gaudin and Wible, 2006 character 16).

(12) Position of mandibular foramen relative to the dorsal margin of the last mandibular dental alveolus: nearly aligned or dorsal (0); ventral (1). (Fernicola, 2008, character 11).

(13) *Distance between the mandibular foramen and the posterior border of the last mandibular alveolus: ≥4 LLM alveolus length (0); <4, ≥1 LLM alveolus length (1); <1 LLM alveolus length (2). (Modified from Fernicola, 2008, character 12).

(14) Orientation of the condyloid process of mandible: dorsal (0); anterodorsal (1). (Fernicola, 2008, character 13).

(15) *Medial projection of the mandibular symphysis: absent or rudimentary (0); present in its ventral half (1); present in its entire length (2). (Fernicola, 2008, character 14).

(16) Medioventral projection of the angular region of mandible: absent (0); present (1). (Fernicola, 2008, character 15).

(17) Marked rugosity on the lateral surface of the angular region: absent (0); present (1). (Fernicola, 2008, character 16).

(18) *Base of the coronoid process of mandible: <70% of the coronoid process height (0); ≥70%, <100% of the coronoid process height (1); basis ≥100% of the coronoid process height (2). (Modified from Fernicola, 2008, character 17).

(19) *Number of lower teeth: eight (0); nine (1); ten or more (2). (Fernicola, 2008, character 18).

(20) Length of the lower toothrow: short, ≤50% of the total length of the mandible (0); elongate, >50% of the total length of the mandible (1). (Modified from Fernicola, 2008, character 19).

(21) *Shape of the last four lower molariforms: circular or elliptical (0); trilobed, with circular or elliptical mesial-most lobule (1); trilobed, with triangular mesial-most lobule (2). (Modified from Fernicola, 2008, character 20).

(22) Premaxillary teeth: absent (0); present (1). (Fernicola, 2008, character 21).

(23) *Number of maxillary teeth: seven (0); eight (1); nine (2). (Fernicola, 2008, character 22).

(24) *Shape of the occlusal surface of the upper toothrow: V-shaped with dorsal apex on all teeth but the last two teeth (0); oblique at the first tooth and flat at the last tooth (1); flat on all tooth (2). (Fernicola, 2008, character 23).

(25) Secondary orthodentine occlusal ramifications: absent (0); present (1). (Fernicola, 2008, character 3).

(26) Shape of the first maxillary molariform: mesiodistal axis $>$ bucolingual (0); mesiodistal axis $\leq$ the buccolingual (1). (Modified from Fernicola, 2008, character 25).

(27) *Shape of the maxillary molariforms: all elliptical (0); the last four trilobed (1); the last five trilobed (2); the last six trilobed (3); the last seven or all trilobed (4). (Fernicola, 2008, character 26).

(28) *Maximum width of the external nasal aperture (MWNA) relative to the LUM: MWNA $<$ lingual width between LUM (0); MWNA $\geq$ lingual width between the LUM, $<$ buccal width between the LUM (1); MWNA $>$ buccal width between the LUM (2). (Modified from Fernicola, 2008, character 27).

(29) *Maximum width of the external nasal apertures relative to the width between the lateral margins of the occipital condyles: $<50\%$ (0); $\geq 50\%$, $<100\%$ (1); $>$ width of the occipital condyles (2). (Modified from Fernicola, 2008, character 28).

(30) Shape of caudal nasal apertures: U-shaped (0); V-shaped (1); lageniform (2). (Modified from Fernicola, 2008, character 29).

(31) *Width of the posterior nasal aperture: $<75\%$ of the height (0); $>75\%$, $<100\%$ of the height (1); width $>$ height (2). (Modified from Fernicola, 2008, character 30).

(32) Position of the anterior border of the squamosal relative to the sphenorbital fissure: posterior (0); in line or anterior (1). (Fernicola, 2008, character 31).

(33) Exposure of the ethmoid in the orbital wall: present (0); absent (1). (Fernicola, 2008, character 32).

(34) Maxillary foramen in lateral view: completely visible (0); partially or not visible (1). (Fernicola, 2008, character 33).

(35) Maxillary foramen in ventral view: visible (0); not visible (1). (Fernicola, 2008, character 34).

(36) Position of the foramen ovale relative to the glenoid fossa: in line (0); posterior (1). (Fernicola, 2008, character 35).

(37) Transverse foramen: present (0); absent (1). (Fernicola, 2008, character 36).

(38) Position of foramen ovale relative to the maxillary foramen: ventral or at the same level (0); dorsal (1). (Fernicola, 2008, character 37).

(39) Relative position of the ventral borders of the maxillary and infraorbital foramina: ventral or at the same level (0); maxillary foramen dorsal (1). (Fernicola, 2008, character 38).

(40) *Position of the medial wall of the infraorbital foramen relative to the labial border of the upper toothrow: in line or medial (0); slightly lateral (1); lateral (2). (Fernicola, 2008, character 39).

(41) Relative position of the lateral borders of the infraorbital and maxillary foramina: infraorbital more medial (0); infraorbital aligned or more lateral (1). (Fernicola, 2008, character 40).

(42) Position of the lacrimal foramen relative to the lateral wall of infraorbital foramen: lateral (0); in line or medial (1). (Modified from Fernicola, 2008, character 41).

(43) Infraorbital foramen in lateral view: visible (0); not visible (1). (Fernicola, 2008, character 42).

(44) Number of molariforms posterior to the infraorbital foramen: ≤ 5 (0); >5 (1). (Modified from Fernicola, 2008, character 43).

(45) Position of the infraorbital foramen relative to the ventral border of the orbit: dorsal or slightly ventral (0); clearly ventral (1). (Fernicola, 2008, character 44).

(46) *Development of the descending process of the zygomatic relative to the length of the upper toothrow: poorly developed (0); developed, $<60\%$ of the total length of the upper toothrow (1); developed, $>60\%$, $<80\%$ of the total length of the upper toothrow (2); strongly developed, $>80\%$ of the total length of the upper toothrow (3). (Modified from Fernicola, 2008, character 45).

(47) *Lateral side of the descending process of zygomatic arch relative to the medial one: lateral side shorter (0); equal (1); lateral side longer (2). (Fernicola, 2008, character 46).

(48) Shape of palate in lateral view: straight or concave (0); sigmoid (1). (Fernicola, 2008, character 47).

(49) Shape of palate posterior to the incisive foramina: flat or gently elevated (0); strongly elevated, partially hides the incisive foramina (1). (Fernicola, 2008, character 48).

(50) *Position of the anterior border of the first maxillary alveolus relative to the posterior plane of the incisive foramina: posterior by more than one and a half times the palatal premaxillary width (0); posterior by more than half the palatal premaxillary width and less than one and half times the same width (1); in line or posterior by less than half the palatal premaxillary width (2); clearly anterior (3). (Fernicola, 2008, character 49).

(51) *Position of the anterior plane of the posterior nasal aperture relative to the upper toothrow, measured as LUM lengths: posterior by >2 LUM lengths (0); posterior by >1 LUM length but <2 LUM lengths (1); anterior or posterior by <1 LUM length (2). (Fernicola, 2008, character 50).

(52) Position of the anterior vascular foramina of palate relative to the anterior border of the upper toothrow: anterior to the posterior border of the first molariform (0); posterior to the first molariform (1). (Fernicola, 2008, character 51).

(53) Strong dorsoventral development of the palatal portion of the premaxilla: absent (0); present (1). (Fernicola, 2008, character 52).

(54) Inclination of the anterior border of premaxilla: does not reach the upper toothrow (0); reaches the toothrow (1). (Fernicola, 2008, character 53).

(55) *Position of the anterior plane of the nasals relative to the anteroventral plane of the premaxilla: anterior (0); in line (1); posterior (2). (Fernicola, 2008, character 54).

(56) *Position of the anterior border of the nasal bones relative to the lacrimal foramen and the ventral border of the orbit: dorsal to the lacrimal foramen (0); between the lacrimal foramen and the ventral border of orbit (1); ventral to the ventral border of the orbit (2). (Fernicola, 2008, character 55).

(57) Position of the posterior plane of the nasals relative to the lacrimal foramina: anterior (0); posterior (1). (Fernicola, 2008, character 56).

(58) Position of the septal process of nasal relative to the anterior border of nasals: at the level or posterior (0); anterior (1). (Fernicola, 2008, character 57).

(59) *Ratio of length of rostrum to width between the lacrimal foramina: >1.5 (0); ≥ 1, <1.5 (1); <1 (2). (Modified from Fernicola, 2008, character 58).

(60) Position of the ventral border of pterygoid relative to the last upper molariform: medial to the labial border of the last upper molariform (0); in line or lateral to the labial

border of the last upper molariform (1). (Fernicola, 2008, character 59).

(61) Rugose portion of pterygoid or pterygoid + alisphenoid: ends posteriorly to the last upper molariform (0); ends at the level of the last molariform (1). (Fernicola, 2008, character 60).

(62) *Separation between the insertion scars of the rectus capitis: widely separated (0); gently separated (1); in contact with a medial crest (2). (Fernicola, 2008, character 61).

(63) *Position of the glenoid fossa relative to the occipital condyle: dorsal (0); at the same level (1); ventral (2). (Fernicola, 2008, character 62).

(64) Ratio of mediolateral width/anteroposterior length of the glenoid fossa: <2 (0); ≥ 2 (1). (Modified from Fernicola, 2008, character 63).

(65) *Position of the glenoid fossa relative to the upper toothrow: posterior by more than eight molariform lengths (0); posterior by more than two molariform lengths (1); posterior by more than one molariform length and less than two (2); posterior by less than one molariform length (3). (Fernicola, 2008, character 64).

(66) Position of the posterior border of the zygomatic relative to the glenoid fossa: at the same level (0); anterior (1). (Fernicola, 2008, character 65).

(67) Shape of the zygomatic-squamosal suture in lateral view: straight (0); L-shaped (1); S-shaped (2). (Fernicola, 2008, character 66).

(68) *Orientation of the long axis of the jugal-squamosal suture: anteroventral (0); ventral (1); posteroventral (2). (Modified from Fernicola, 2008, character 67).

(69) Position of the lateral plane of the zygomatic process of squamosal relative to the lateral plane of the lacrimal: in line or medial (0); lateral (1). (Fernicola, 2008, character 68).

(70) Dorsal superposition jugal/squamosal in lateral view: absent (0); present (1). (Fernicola, 2008, character 69).

(71) Sagittal crest: absent or poorly developed (0); present (1). (Fernicola, 2008, character 70).

(72) *Descending laminae of frontal: absent (0); present, not ventrally developed (1); present, ventrally developed (2). (Fernicola, 2008, character 71).

(73) Orientation of the descending laminae of frontal relative to the anteroposterior axis of skull: $<45^\circ$ (0); $\geq 45^\circ$ (1). (Modified from Fernicola, 2008, character 72).

(74) Position of the posterior-most plane of frontal relative to the glenoid fossa: anterior or in line (0); posterior (1). (Fernicola, 2008, character 73).

(75) *Position of lacrimal foramen relative to the occipital condyle: dorsal (0); at the same level (1); ventral (2). (Fernicola, 2008, character 74).

(76) *Position of the lacrimal foramen: closer to the palate (0); nearly midway between the palate and the dorsal side of skull (1); closer to the dorsal side of skull (2). (Fernicola, 2008, character 75).

(77) Position of the lacrimal foramen relative to the anterior edge of the orbit: outside the orbit (0); inside the orbit (1). (Fernicola, 2008, character 76).

(78) *Bone surface dorsal to the lacrimal foramen: smooth (0); irregular and strongly punctuated (1); conical and strongly developed (2). (Fernicola, 2008, character 77).

(79) *Zygomatic process of frontal: absent or rudimentary (0); well developed (1); strongly developed (2). (Fernicola, 2008, character 78).

(80) Shape of orbit: rectangular (0); U-shaped (1); circular (2). (Fernicola, 2008, character 79).

(81) Width of the occipital condyles: width = height or width > height (0); width < height (1). (Fernicola, 2008, character 80).

(82) *Angle between the occipital plane and the horizontal plane of the skull: $\geq 80^\circ$ (0); $<80^\circ$, $\geq 65^\circ$ (1); $<65^\circ$, $\geq 45^\circ$ (2); $<45^\circ$ (3). (Modified from Fernicola, 2008, character 81).

(83) Ratio of postorbital minimum width of skull relative to the width between the lateral margins of occipital condyles: <1.2 (0); ≥ 1.2 (1). (Modified from Fernicola, 2008, character 82).

(84) Occipital crest: absent or ends at the dorsal third of occipital (0); ends at the ventral third of occipital (1). (Fernicola, 2008, character 83).

(85) Neural process of atlas: poorly developed (0); well-developed (1). (Porpino et al., 2009, character 1).

(86) Separation between the atlantal foramina of atlas: narrow, $<50\%$ of the maximum transverse diameter of the atlas (0); wide, $>50\%$ of the maximum transverse diameter of the atlas (1). (Porpino et al., 2009, character 7).

(87) Shape of the neural canal of the atlas: dorsal half wider (0); ventral half wider (1); nearly isodiametric (2). (Porpino et al., 2009, character 4).

(88) Lateral edge of the transverse process of atlas in dorsal view: projected laterally beyond the lateral borders of the articular facet for the occipital condyles (0); nearly aligned with the lateral borders of the articular facet for the occipital condyles (1). (Porpino et al., 2009, character 9).

(89) *Position of the transverse foramen of atlas relative to the neural canal: inside the canal (0); lateral, closer to the canal than to the basis of the transverse process (1); lateral, nearly midway between the canal and the basis of the transverse process (2); lateral, closer to the basis of the transverse process than to the canal (3). (Porpino et al., 2009, character 8).

(90) Position of the transverse foramen of atlas relative to the articular facet for the axis: dorsally (0); dorsolaterally (1). (Modified from Porpino et al., 2009, character 2).

(91) Orientation of the major axis of the articular facet for the axis: mediolateral (0); dorsoventral (1). (Porpino et al., 2009, character 3).

(92) Ventral projections of the transverse process of atlas: present (0); absent (1). (Porpino et al., 2009, character 5).

(93) Angle between the caudal border of scapula and the dorsoventral axis of the scapular spine: $<90^\circ$ (0); nearly 90° (1).

(94) Shape of the humeral head: elongated craniocaudally (0); nearly rounded (1).

(95) Lesser tuberosity of humerus: well-developed (0); moderately or poorly developed (1). (Porpino et al., 2009, character 13).

(96) Humeral tuberosity for the m. teres major: absent (0); present (1).

(97) Lateral edge of the capitulum of humerus: forms a crest for articulation with the lateral facet of the proximal epiphysis of the radius (0); does not form a crest (1). (Porpino et al., 2009, character 9).

(98) Shape of the distal end of the deltopectoral shelf of humerus: rounded (0); narrows to a point distally (1). (Porpino et al., 2009, character 10).

(99) Length of the deltopectoral shelf of humerus: long, $\geq 50\%$ of the total length of the humerus (0); short, $<50\%$ of the total length of the humerus (1). (Porpino et al., 2009, Character 11).

(100) Coronoid fossa of humerus: absent or poorly demarcated (0); deep (1). (Porpino et al., 2009, character 12).

(101) *Supinatory crest of humerus: poorly developed, maximum humeral width at the greatest lateral extension of the supinatory crest $<60\%$ of the maximum width at the epicondyles (0); moderately developed, width at the greatest lateral extension of the supinatory crest 60–70% of the

maximum width at the epicondyles (1); well developed, width at the greatest lateral extension of the supinatory crest >70% of the maximum width at the epicondyles (2). (Porpino et al., 2009, character 12).

(102) Distal-most portion of the medial malleolus of radius in cranial view: extending distally relative to the distal end of the lateral malleolus (0); at the same level relative to the distal end of the lateral malleolus (1). (Porpino et al., 2009, character 17).

(103) Position of the greater trochanter of femur: projected above the level of head (0); at nearly the same level or just below the level of head (1). (Porpino et al., 2009, character 18).

(104) Orientation of the greater trochanter of femur: parallels the major axis of femur (0); laterally oriented (1). (Porpino et al., 2009, character 25).

(105) Orientation of the head of femur: medially oriented (0); proximally oriented (1). (Porpino et al., 2009, character 24).

(106) Shape of lesser trochanter of femur: tubercle continued by a crest extending distally; (0); tubercle without a crest extending distally (1). (Porpino et al., 2009, character 21).

(107) Position of lesser trochanter relative to the head of femur in medial view: lesser trochanter strongly projected caudally (0); lesser trochanter nearly aligned with head (1). (Porpino et al., 2009, character 23).

(108) Cranial depression between the head and greater trochanter of femur: absent or poorly defined (0); clearly demarcated (1). (Porpino et al., 2009, character 26).

(109) *Position of the third trochanter of femur: slightly above or near midshaft (0); just below midshaft (1); displaced to the distal end (2). (Porpino et al., 2009, character 19).

(110) Suprapatellar fossa of femur: absent or very shallow (0); deep (1). (Porpino et al., 2009, character 20).

(111) Relative development of the crests of patellar surface of femur: nearly symmetrical (0); asymmetrical, medial crest strongly projected cranially (1). (Porpino et al., 2009, character 22).

(112) Extension of the tibial crest of tibia-fibula: reaching the midshaft distally (0); extending distally beyond midshaft (1). (Modified from Porpino et al., 2009, character 27).

(113) *Transverse diameter of the proximal end of tibia-fibula: narrow, <35% of total length of the tibial portion of tibia-fibula (0); intermediate, 35–50% of total length of the tibial portion of tibia-fibula (1); wide, >50% of total length of the tibial portion of tibia-fibula (2). (Porpino et al., 2009, character 29).

(114) Transverse diameter of the proximal epiphysis of tibia-fibula relative to the transverse diameter of its distal epiphysis: proximal < distal (0); proximal > distal (1). (Porpino et al., 2009, character 30).

(115) Distal border of the lateral malleolus of tibia-fibula: nearly at the same level of distomedial border (0); projected distally beyond the distomedial border (1). (Porpino et al., 2009, character 28).

(116) Shape of the ectal facet of calcaneum: oblong (0); nearly triangular (1). (Porpino et al., 2009, character 31).

(117) Major axis of ectal facet: 45° relative to the long axis of calcaneum (0); <45° relative to the long axis of calcaneum (1). (Porpino et al., 2009, character 32).

(118) Interarticular sulcus between the astragalar facets of calcaneum: shallow (0); deep (1). (Porpino et al., 2009, character 34).

(119) Groove for the calcaneal tendon of the m. gastrocnemius: elongated and narrow (0); short and wide (1). (Porpino et al., 2009, character 37).

(120) Shape of the tuber of calcaneum: thin, maximum width <60% of the length (0); robust, maximum width >60% of the length (1). (Porpino et al., 2009, character 44).

(121) Neck of calcaneum: long, length of the neck/total length ≥ 1.5 (0); short, length of the neck/total length < 1.5 (1). (Porpino et al., 2009, Character 33).

(122) Peroneal tubercle of calcaneum: absent or rudimentary (0); present, well-developed (1). (Porpino et al., 2009, character 36).

(123) *Transverse width of calcaneum at the level of astragalar facets: narrow, <50% of total length (0); wide 50–60% of total length (1); very wide, >60% of total length (2). (Porpino et al., 2009, character 38).

(124) Fibular facet of calcaneum: absent (0); present (1). (Porpino et al., 2009, character 39).

(125) Length between the dorsal border of cuboid facet and the distal margin of ectal facet of calcaneum: short, <45% of the total length of calcaneum (0); long, 45–55% of total length of calcaneum (1). (Porpino et al., 2009, character 40, modified).

(126) *Calcaneal groove for the tendon of m. peroneous brevis: absent (0); present, poorly developed (1); present, well-developed (2). (Porpino et al., 2009, character 41).

(127) Sustentaculum of calcaneum: thin, dorsoplantar diameter <50% of the transverse diameter (0); robust, dorsoplantar diameter >50% of the transverse diameter (1). (Porpino et al., 2009, character 42).

(128) Shape of the end of sustentacular process of calcaneum: sharp (0); rounded (1). (Porpino et al., 2009, character 43).

(129) Transverse diameter of the cuboid facet of calcaneum: ≤ dorsoventral diameter (0); > dorsoventral diameter (1). (Porpino et al. 2009, character 35).

(130) Navicular tuberosity of astragalus: absent (0); present (1).

(131) Crests of astragalar trochlea: lateral crest gently higher or nearly at the same level (0); lateral crest much higher than the medial one (1).

(132) Shape of sustentacular facet of astragalus: oblong (0); nearly circular (1).

(133) Proximomedial tuberosity of astragalus: poorly developed (0); well developed (1).

(134) Groove between the mediodistal edge of the sustentacular facet and the plantar edge of the navicular facet of the astragalus: present (0); absent (1).

(135) Relative position between the mediodistal edge of the medial trochlear crest and the proximomedial edge of the navicular facet of astragalus: in line (0); clearly dorsal (1).

(136) Relative position of the proximal edges of ectal and sustentacular facets of astragalus: proximal edge of the ectal facet higher (0); at the same height (1).

(137) Sustentacular facet of astragalus: concave (0); flat to slightly convex (1).

(138) *Height at the medial portion of astragalus: high, >90% of the maximum width of astragalus (0); intermediate, <90%, >80% of the maximum width of the astragalus (1); short, <80% of the maximum width of astragalus (2).

(139) *Astragalar neck: long (0); short (1); very short (2).

(140) Shape of ectal facet of astragalus: oblong (0); nearly triangular (1).

(141) Proximodistal length of the ectal facet relative to the sustentacular facet: nearly equal (0); ectal clearly longer than the sustentacular (1).

(142) Navicular articular facet for the plantar sesamoid: present (0); absent (1). (Porpino et al., 2009, character 45).

(143) Shape of the navicular facet for the cuboid: short, dorsoplantar diameter < twice proximodistal diameter (0); elongated, dorsoplantar diameter > twice proximodistal diameter (1). (Porpino et al., 2009, character 46).

(144) Shape of the navicular facet for the astragalus: lageniform (0); nearly triangular, with rounded edges (1). (Porpino et al., 2009, character 47).
(145) Position of the navicular facet for the lateral cuneiform: perpendicular to the facets for the intermediate and medial cuneiforms (0); parallels the facets for the intermediate and medial cuneiforms (1). (Porpino et al., 2009, character 48).
(146) Composition of caudal armor: formed by rings of osteoderms exclusively (0); rings plus well-developed caudal tube (1).
(147) Conical tubercle in the lateral and terminal figures of caudal tube: absent (0); present (1).
(148) Number of lateral figures of caudal tube: ≥2 (0); 1 (1).
(149) *Length of L1 relative to the length of terminal figure of caudal tube: length of L1 <90% of the length of terminal figure (0); length of L1 >90%, <100% of the length of terminal figure (1); length of L1 > length of terminal (2).
(150) Terminal figures of caudal tube: contact or nearly contact each other dorsally (0); clearly separated dorsally (1).
(151) Dorsoventral diameter of L1: clearly < the dorsoventral diameter of caudal tube at its corresponding region (0); nearly matches the dorsoventral diameter of the caudal tube at its corresponding position (1).

APPENDIX 3. The scoring of the 151 characters for the 17 terminal taxa used in phylogenetic analysis. States marked with a question mark are missing and with N are inapplicable; polymorphic character states within a single taxon are represented by A (0/1), B (1/2) and C (2/3).

Dasypus
```
0000000000 0000000000 00A0?00000 0100100100
000000?000 0000020000 0210000000 00N0010000
0001000000 0000100100 0000000000 0000000000
0001010000 0000000000 000000NNNN N
```
Eutatus
```
0121001200 1011000110 0020?00100 001110AA01
10A000?000 200002O?00 0200101010 00N0020201
0000000010 00?0000000 0000000100 001000??10
0101100000 0?0001010? ?0??00NNNN N
```
Euphractus
```
2111101200 1011001121 0110?00000 0A10000001
000000?001 2100020010 010010AA10 00N0100102
0000000000 0000000000 0000000101 0100001010
0100100110 0000000010 100000NNNN N
```
Pampatherium
```
2221101100 2121101111 1111002210 0011000A01
101000?002 1110010011 0101110010 1100010101
0000111110 0000100100 0001101101 1???000100
0001011100 0001100100 0?0?00NNNN N
```
Pachyarmatherium
```
?????????? ?????????? ?????????? ??????????
?????????? ?????????? ?????????? ??????????
????101010 01?0110010 0001101100 0110000000
100102000? ?????????? ?0000????? ?
```
Propalaehoplophorus
```
2222110211 2121210101 1012011112 1111000112
1110011103 210011??21 1211212111 1200120B11
010A1?1??0 0000100110 1001101?10 1?110???01
11?00211?1 0111001111 1??1?0??NN N
```
Eucinepeltus
```
?C2?11???? 2???21??0? 1012011112 1111000102
1110011103 2100111??1 1211212111 1200120211
?101?????? ?????????? ?????????? ??????????
?????????? ?????????? ?????0NNNN N
```
Glyptodon
```
1232110211 2121200201 2012104211 1111011112
11A1022112 2100111021 10B1312110 1200B20112
0300012121 1111111111 2111111021 1021000111
1020121101 0010110220 011110NNNN N
```
Doedicurus
```
1222110211 2121200201 2012A03210 1111011112
11A103B103 2100111021 0221312111 120?220122
0300012121 1111101110 2111111021 102?100101
1120021101 0000000220 0111110100 0
```
Plohophorus
```
?????????? ?????????? ??120?3??0 1?11011112
10110??1?? 21???????? ?1113???1? 1200220201
1300?????? ?????????? ?????????? ??????????
?????????? ?????????? ?????10000 0
```
Urotherium
```
??3?1????? ????2????? 2012004210 1111011112
101102?10? 21?0?1??21 ??B1312111 0200220201
1201?????? ?????????? ?????????? ??????????
?????????? ?????????? ?????10A00 0
```
Panochthus
```
1332110211 2121200201 2012104220 2111011112
1001132102 21112B1121 1BA13???1? 0211A21B21
1310111121 1001101101 2111111021 11?1111101
1110021111 1101001121 1101111021 1
```
Neosclerocalyptus
```
1332110211 2121200201 2012003220 2111011112
10A1132112 2111201121 1B11312111 A21AA21211
A211111121 1001110101 2001101021 1121111101
1110021111 1101001121 1101110000 0
```
Pseudoplohophorus
```
?232110211 2121210201 2012013210 1?11011112
1011022102 210011??21 12113???1? ?20?120211
1301?12121 1??010?1?? ?????????? ??????????
?????????? ?????????? ?????10000 0
```
Eosclerocalyptus
```
?????????? ?????????? ?012012210 2111011112
1011010102 210011??21 1?113???1? 120?120211
12010?2?21 10???????? ?????????? ??????????
?????????? ?????????? ?????10000 0
```
Hoplophractus
```
??3??????? ?12??1???? 2012013210 1111011112
11100??10? 2100?1???1 12113???1? 1200120211
??010?1110 0?????1??0 ??1110??11 ?????00?0?
11?002?1?1 0010001111 0????10000 0
```
Stromaphorus
```
?22211???1 212?210?01 201?0?CB10 1111011112
11100??10? 2100111?21 1211312111 1200?2011?
1201?????? ?????????? ?????????? ??????????
?????????? ?????????? ?????10020 0
```
Hoplophorus
```
?????????? ?????????? ????004??? ???10111?2
??1?1??1?? ?1???????? ?20?????1? 12100??211
0201?????? ??00101101 21?1????21 ??????????
?????????1 1001101121 0111111111 1
```